



Technical Memorandum 86050

**Goddard Space Flight Center  
Contributions to the University  
of California, Santa Cruz Summer  
Workshop on "High Energy  
Transients" (July 1983)**

**R. Ramaty, R. J. Murphy, T. L. Cline,  
B. J. Teegarden, J. P. Norris, U. D. Desai,  
A. K. Harding, B. E. Schaefer,  
T. T. von Roseninge and R. Kaipa**

**OCTOBER 1983**

National Aeronautics and  
Space Administration

**Goddard Space Flight Center**  
Greenbelt, Maryland 20771

Goddard Space Flight Center  
Contributions to the  
University of California, Santa Cruz Summer Workshop on  
"High Energy Transients"  
(July 1983)

to be published in

The American Institute of Physics Conference Proceedings, 1984

October 1983

The GSFC Contributions to the University of California,  
Santa Cruz Summer Workshop on  
High Energy Transients

July 1983

Table of Contents:

Neutrons and Gamma Rays from Solar Flares R. Ramaty and R. J. Murphy.....	1
Gamma Ray Bursts: A 1983 Overview T. L. Cline.....	15
The Spectral Properties of Gamma Ray Bursts: A Review of Recent Developments B. J. Teegarden.....	25
Frequency of Fast, Narrow Gamma Ray Bursts and Burst Classification J. P. Norris, T. L. Cline, U. D. Desai and B. J. Teegarden.....	41
Equilibria in Strongly Magnetized Pair Plasmas Alice K. Harding.....	47
Implications of the Three GRB Optical Flashes B. E. Schaefer.....	51
The Rapidly Moving Telescope: An Instrument for the Precise Study of Optical Transients R. J. Teegarden, T. T. von Roseninge, T. L. Cline, and R. Kaipa...	55

## NEUTRONS AND GAMMA RAYS FROM SOLAR FLARES

R. Ramaty and R. J. Murphy\*  
 Laboratory for High Energy Astrophysics  
 Goddard Space Flight Center, Greenbelt, MD. 20771

### ABSTRACT

The theory of neutron and gamma-ray production in flares is reviewed and comparisons of the calculations with data are made. The principal conclusions pertain to the accelerated proton and electron numbers and spectra in flares and to the interaction site of these particles in the solar atmosphere. For the June 21, 1980 flare, from which high-energy neutrons and high-energy ( $>10$  MeV) photons were seen, the electron-to-proton ratio is energy dependent and much smaller than unity at energies greater than 1 MeV. The interaction site of these particles appears to be the solar chromosphere.

### INTRODUCTION

Interactions in the solar atmosphere of flare-accelerated protons, alpha particles and heavier nuclei produce observable gamma-ray lines and neutrons. The detection of this neutral radiation provides unique information on particle acceleration and interaction processes, on the flare mechanism and on properties of the solar atmosphere.

Energetic particle interactions produce a variety of secondary products. For solar flares, the most important of these are neutrons, excited and radioactive nuclei, and  $\pi$  mesons. Solar neutrons are observed both directly at the Earth and in the 2.223 MeV line from neutron capture on hydrogen in the photosphere. Detectable gamma-ray lines are also produced by the deexcitation of nuclear levels and by the annihilation of positrons from the decay of radioactive nuclei and  $\pi^+$  mesons. The decay of  $\pi^0$  mesons could lead to observable  $>10$  MeV gamma-ray emission, but it appears that for solar flares most of the emission at these energies is due to relativistic electron bremsstrahlung.

Gamma-ray lines from solar flares were first observed<sup>1</sup> with a NaI spectrometer flown on OSO-7. Following these observations, solar gamma-ray lines were seen with the NaI spectrometer on HEAO-1<sup>2</sup>, the NaI spectrometer on SMM<sup>3,4,5</sup>, the high-resolution Ge spectrometer on HEAO-3<sup>6</sup>, and the CsI spectrometer on HINOTORI<sup>7</sup>. Gamma rays of energies  $>10$  MeV and high-energy solar neutrons near Earth were detected<sup>8,9</sup> with the gamma-ray spectrometer on SMM. The production of solar neutrons in flares was recently inferred from observations<sup>10</sup> of the decay protons in interplanetary space and from ground based observations<sup>9</sup>. The theory of gamma-ray and neutron

\*Also Physics Department, University of Maryland, College Park, MD. 20742

production in flares was reviewed<sup>11</sup> recently.

Comparisons of gamma-ray observations from flares and charged-particle measurements in the interplanetary medium have shown<sup>12,13</sup> that gamma-ray production in solar flares takes place predominantly during the slowing-down of the accelerated particles in the solar atmosphere, rather than during their acceleration or escape from the Sun. This is reasonable since particle acceleration generally requires a low ambient density so that the acceleration rate exceeds the energy-loss rate, whereas effective nuclear interactions require an ambient density that is high enough to stop the particles. Thus, we expect the region of most efficient acceleration to be above the interaction region where the observed neutrons and gamma rays are produced. This model of nuclear interactions is commonly referred to as the thick-target model.

In the present paper we review the most important aspects of neutron, gamma-ray line and gamma-ray continuum production in solar flares and we summarize the implications of the comparisons of these calculations with data.

## NEUTRONS

As just mentioned, solar neutrons are observed in the 2.223 MeV line and are directly detected at the Earth. The 2.223 MeV line was predicted theoretically<sup>14</sup> to be the strongest line from flares and this prediction was confirmed by observations<sup>1,2,4</sup>. The limb darkening of the 2.223 MeV line caused by Compton scattering in the photosphere<sup>15</sup>, has also been observed<sup>4,7</sup>. This effect, together with the time delay of the flux in this line<sup>3,16</sup>, and the precisely determined line energy<sup>6,17</sup>, provides clear evidence that the observed emission at 2.223 MeV is indeed due to neutron capture and that this capture takes place in the photosphere. Neutron capture on H, the process which forms the observed line, must compete with capture<sup>15</sup> on  $^3\text{He}$ , a process with a very large cross section that produces no photons. Observations of the 2.223 MeV line from solar flares, therefore, provide information on the photospheric  $^3\text{He}$  abundance.

For solar flares whose duration is much shorter than the typical neutron transit time from the Sun to Earth, the observed time dependence of the neutron flux is a direct measure of the energy spectrum of the neutrons released from the Sun. This spectrum, in turn, depends on the energy spectrum and angular distribution of the accelerated particles, as well as on the interaction model of these particles with the solar atmosphere. The recent high-energy neutron observations<sup>8,9</sup> confirm the overall time dependence of the neutron flux at Earth predicted earlier<sup>14,18</sup>. These previous neutron production calculations have recently been extended<sup>11,19</sup> and the results have been compared with the observations. We now summarize these studies and also present hitherto unpublished calculations.

The thick-target model was used to calculate the production of neutrons at the Sun. The energy spectrum of the protons and nuclei

that emerge from the acceleration region and are incident on the interaction region,  $N(E)$ , was assumed to be either a power law,  $N(E) \propto E^{-s}$ , or a Bessel function,  $N(E) \propto K_2[2(3p/(m\alpha T))^{1/2}]$ , where  $E$  and  $p$  are particle energy and momentum per nucleon, respectively, and  $m$  is the proton mass. The power law is a useful mathematical expression, but it does not relate to any particular acceleration mechanism. The Bessel function represents the spectrum of nonrelativistic particles resulting from stochastic Fermi acceleration<sup>20,21</sup> with rate coefficient  $\alpha$  and particle residence time in the acceleration region  $T$ . The product  $\alpha T$  characterizes the particle spectrum, such that a larger value of  $\alpha T$  corresponds to a harder spectrum.

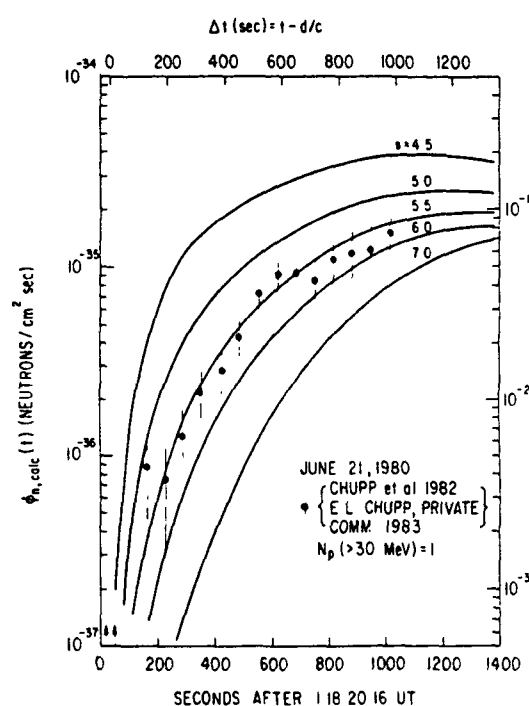


Fig. 1. Observed and calculated neutron fluxes at Earth for power-law proton spectra with spectral index  $s$  as functions of the difference between the Sun-Earth transit times of neutrons and photons.

from a limb flare would be larger than from a disk flare. There are, however, as yet no data to suggest such an anisotropy.

Using a detailed study of neutron production cross sections and angular distributions, neutron production spectra were evaluated for various energetic particle spectra. The resultant time-dependent neutron fluxes at Earth depend on these spectra, on the time profile of the neutron production at the Sun, on the amount of attenuation suffered by the neutrons in the solar atmosphere and on the decay of

It was assumed, in addition, that the composition of the accelerated particles is the same as that of the solar photosphere and that the protons and nuclei have the same energy spectrum. These particles were then allowed to slow down in the interaction region due to ionization losses in a neutral medium. For simplicity, it was also assumed that within the interaction region the angular distribution of the charged particles is isotropic. An anisotropic distribution would have observable effects. For example, if the protons and nuclei were preferentially directed downward toward the photosphere, the neutron flux

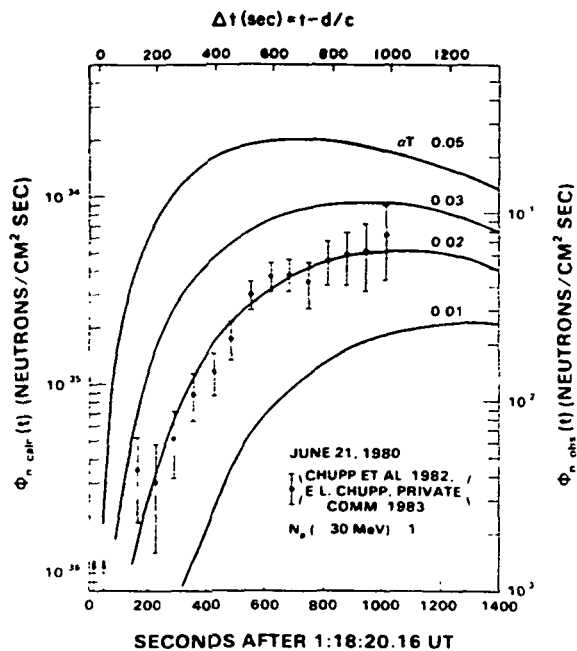


Fig. 2. Observed and calculated neutron fluxes at Earth for Bessel function spectra with spectral parameter  $\alpha T$  as functions of the difference between the Sun-Earth transit times of neutrons and photons.

1:18:55 UT -  $d/c$ , i.e. at the midpoint between the two impulsive photon emission peaks whose centers, shown by arrows, were observed at 1:18:40 and 1:19:10 UT (e.g. ref. 8). Here  $d = 1A.U.$  The total duration of the impulsive phase of the June 21, 1980 flare was approximately 60 sec. As can be seen, the shape of the observed time dependence fits very well those calculated for  $s=5.5$  and  $\alpha T=0.02$ . These spectral parameters pertain to the proton and alpha particle spectrum in the range from about  $10^2$  and  $10^3$  MeV/nucleon. The absolute normalization of the calculations to the data determines the total neutron production,  $N_n$ , and the total number of accelerated protons with energies greater than  $E$ ,  $N_p(>E)$ . In the case of the power law,  $N_n \approx 2.5 \times 10^{31}$  and  $N_p(>30 \text{ MeV}) \approx 5 \times 10^{33}$ , while for the Bessel function,  $N_n \approx 2.8 \times 10^{30}$  and  $N_p(>30 \text{ MeV}) \approx 1.2 \times 10^{33}$ . But, as we shall see in the next section, an unbroken power law extrapolated to energies below 30 MeV is inconsistent with the nuclear line data. On the other hand, since the slope,  $-d \log N / d \log E$ , of the Bessel function decreases with decreasing  $E$ , this spectral form turns out to be consistent with both the neutron and line observations.

The value of  $N_n$  associated with the Bessel function, together

the neutrons in flight.

The calculated time-dependent neutron fluxes at the Earth are shown in Figures 1 and 2, for power laws and Bessel functions, respectively, assuming instantaneous neutron production and free, unattenuated escape from the Sun. The time  $\Delta t$  is that in excess of the light-travel time from the Sun, where  $t$  is measured from the neutron production time. Also shown in these figures is the neutron flux from the June 21, 1980 flare observed down to 50 MeV (ref. 5 and E.L. Chupp, private communication 1983). It was assumed that the neutron production time was at

with the estimated<sup>22</sup> value of 0.23 for the number of observable 2.223 MeV photons per neutron from a disk-centered flare, implies a 2.223 MeV line fluence of  $\sim 230$  photons/cm<sup>2</sup> at the Earth from such a flare. The fact that the observed (D. Forrest, private communication 1982) 2.223 MeV line fluence for the June 21, 1980 limb flare was only  $\sim 6$  photons/cm<sup>2</sup>, confirms the limb-darkening of this line.

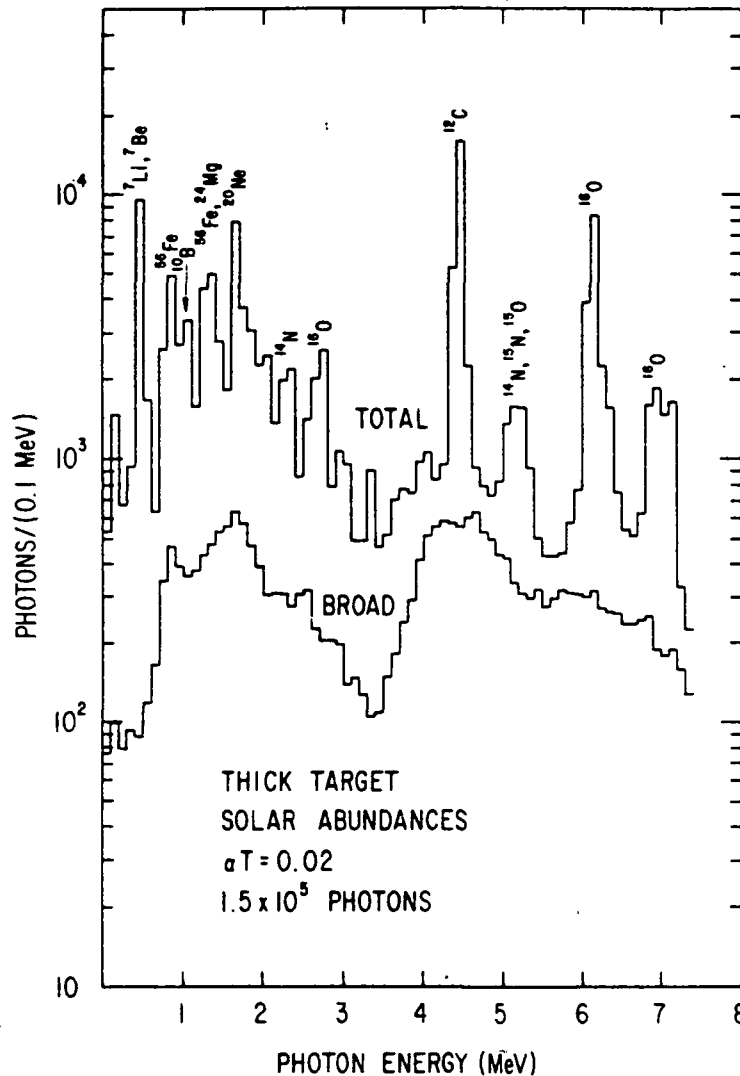
The assumption of free neutron escape determines the maximum ambient density in the interaction region. If the dependence on height of this density can be approximated by an exponential with scale height  $h_0$ ,  $n(h) = \exp(-h/h_0)$ , then for a limb flare the observable neutron flux originating at a height  $h$  is attenuated by approximately  $\exp[-((\pi/2)Rh_0)^{1/2}\sigma n(h)]$ , where  $R$  is the solar radius and  $\sigma$  is the neutron-proton elastic scattering cross section. Since  $\sigma$  increases with decreasing neutron energy, the maximum value of  $n(h)$  consistent with free neutron escape is determined by the lowest observed neutron energy, approximately 50 MeV (ref. 8). For  $h_0 = 10^7$  cm, we find that  $n < 5 \times 10^{15}$  cm<sup>-3</sup>, essentially the top of the photosphere. Since the vertical column depth at this density is<sup>23</sup> only 0.2 g cm<sup>-2</sup>, while the stopping ranges of the protons that produce the neutrons are greater than 5 g cm<sup>-2</sup>, the protons must be stopped at column depths significantly less than their ranges<sup>19</sup>. This could be achieved perhaps by magnetic mirroring<sup>24</sup> or by scattering from magnetic inhomogeneities.

#### NUCLEAR DEEXCITATION LINES

A variety of gamma-ray lines are produced in solar flares from the deexcitation of nuclear levels<sup>25</sup>. We show in Figure 3 a spectrum derived<sup>11</sup> from a thick-target Monte-Carlo calculation in which the ambient medium has photospheric composition and the energetic particles have a Bessel function spectrum with  $\alpha T = 0.02$ , photospheric composition and isotropic angular distribution. The upper histogram shows the total gamma-ray spectrum, while the lower one shows the broad component, i.e. gamma rays from the interactions of energetic nuclei heavier than helium.

The total spectrum in Figure 3 contains a variety of narrow lines which result mostly from the deexcitation of ambient nuclei excited by fast protons and alpha particles. As can be seen, the strongest such lines are at 6.129 MeV from <sup>16</sup>O, at 4.438 MeV from <sup>12</sup>C, at 1.634 MeV from <sup>20</sup>Ne, at 0.847 MeV from <sup>56</sup>Fe, at  $\sim 1.3$  MeV from <sup>24</sup>Mg and <sup>56</sup>Fe, and at  $\sim 0.45$  MeV from <sup>7</sup>Li and <sup>7</sup>Be. Excited states of Li and Be are formed in solar flares by nonthermal fusion reactions between alpha particles<sup>26</sup>. All of these lines have been seen from solar flares<sup>5,7</sup>.

While the relative widths of these narrow lines, broadened by the recoil velocities of the heavy target nuclei, are only on the order of 1 to 2 percent, the widths of the broad lines, reflecting the velocities of the projectiles themselves, are much larger. Consequently, only a few discrete features can be discerned in the broad component. As can be seen, there is a broad feature between 4



and 5 MeV, mostly from  ${}^{12}\text{C}$ , another one between 1 and 2 MeV from  ${}^{20}\text{Ne}$ ,  ${}^{24}\text{Mg}$ ,  ${}^{28}\text{Si}$  and  ${}^{56}\text{Fe}$ , and a broad line at  $\sim 0.85$  MeV from  ${}^{56}\text{Fe}$ . But the contribution of the broad component to the total emission in Figure 3 is quite small. In thick-target interactions, this is caused by the suppression of the contribution of the heavy nuclei in comparison with that of protons and alpha particles resulting from their larger energy loss rates.

In addition to the nuclear lines shown in Figure 3, gamma-ray emission from flares should also contain a significant contribution from electron bremsstrahlung (see

Fig. 3. Energy spectrum of prompt nuclear deexcitation radiation.

the section on continuum emission). In the 4-7 MeV band, however, most of the emission appears to be  ${}^{27,28}$  nuclear radiation from C, N and O. This result is supported by data<sup>4</sup> which indicate that for all disk flares from which gamma-ray lines were seen, the ratio of the observed fluence in the 4-7 MeV band to the fluence in the 2.223 MeV line does not vary much from one flare to another. This approximate constancy indicates that both radiations are produced by the same population of energetic particles. If one of them were produced by electrons and the other by nuclei, one would expect a much more variable ratio than observed.

The observed 4-7 MeV-to-2.223 MeV fluence ratios provide information on the spectrum of the accelerated protons and nuclei in

the energy range from about 10 to 100 MeV/nucleon. The fact that this ratio does not vary much from flare to flare implies that the particle spectrum in the 10 to 100 MeV/nucleon range also does not change much from one flare to another. Indeed, it has been shown<sup>11,19</sup> that for 7 disk flares  $0.014 < \alpha T < 0.02$ . We find that if the energetic particle spectrum in the 10 to 100 MeV/nucleon range is approximated by a power law, then in the thick-target model, the same data implies  $4 > s > 3$ . The 4-7MeV-to-2.223MeV fluence ratio, however, cannot be used for determining the particle spectra of limb flares, because of the strong attenuation of the 2.223 MeV line in the photosphere.

As we have seen in the section on neutrons, at energies  $> 100$  MeV the proton spectrum can be determined from the observed time dependence of high-energy neutrons and this technique can be used for limb flares. For the June 21, 1980 limb flare, the neutron observations imply  $\alpha T \approx 0.02$  or  $s \approx 5.5$ . Using these spectra, we have calculated the 4-7 MeV fluence from the June 21, 1980 flare and have found that the Bessel function gives a result consistent with the observations<sup>4</sup>, but the power law with  $s \approx 5.5$  implies a 4-7 MeV fluence which exceeds that observed by two orders of magnitude. In addition, the spectrum given by  $\alpha T \approx 0.02$  is consistent with the spectra obtained from the 4-7MeV-to-2.223MeV ratios for disk flares, but the power law with  $s \approx 5.5$  is not. All of these results imply that the solar flare proton spectra are not simple power laws over an extended energy range ( $\sim 10$  MeV to several hundred MeV). Instead, the slope of the spectrum should decrease with decreasing energy, a requirement that is fulfilled by the Bessel function.

A similar result is obtained from observations of energetic protons in interplanetary space<sup>29</sup>. Here Bessel function spectra with  $0.014 < \alpha T < 0.036$  provide a good fit to the observed proton spectra. The fact that similar ranges of  $\alpha T$  are deduced from the gamma-ray and neutron data, on the one hand, and from the interplanetary particle observations, on the other, suggests that the same mechanism accelerates both the energetic particles which remain trapped at the Sun and those which escape into interplanetary space.

#### POSITRONS

The 0.511 MeV line due to positron annihilation has been observed from several solar flares<sup>1,4,30</sup>. Calculations of positron production from the decay of  $\pi^+$  mesons and radioactive nuclei were carried out previously<sup>11</sup>. The initial energies of positrons from radioactive nuclei are of the order of several hundred keV while those from  $\pi^+$  decay are from about 10 to 100 MeV. But because for  $\alpha T = 0.02$  only about  $10^{-3}$  of the total positron production is<sup>11</sup> from  $\pi^+$  decay, the initial energies of the bulk of the positrons are expected to be less than an MeV.

The slowing down of positrons from the energies at which they are produced to energies comparable with those of the ambient electrons where they annihilate, and the subsequent annihilation

process have been studied in considerable detail<sup>22,31,32</sup>. Positrons with an initial energy of  $\sim 0.5$  MeV slow down and annihilate in about  $2 \times 10^{12}/n_H$  sec, where  $n_H$  is the density of the ambient hydrogen. If  $n_H$  is high enough so that the slowing down and annihilation time is much shorter than the half-lives of the dominant positron emitters, the time dependence of the 0.511 MeV line flux is determined only by the decay rates of the positron emitters and their relative contributions to the total positron production. As we shall see, this seems to be the case in solar flares.

If  $n_H$  is sufficiently low ( $<10^{14} \text{ cm}^{-3}$ ), most of the positrons form positronium before they annihilate. Positronium annihilates from its ground state. Parapositronium produces two line photons, while orthopositronium annihilates into three photons, producing a characteristic continuum at energies below  $m_e c^2$ . The quantity  $\bar{f}_{0.511}$ , defined as the average number of 0.511 MeV photons per annihilating positron, is  $\sim 0.65$  if the density is much less than  $10^{14} \text{ cm}^{-3}$  and it is  $>1$  if the density is much higher.

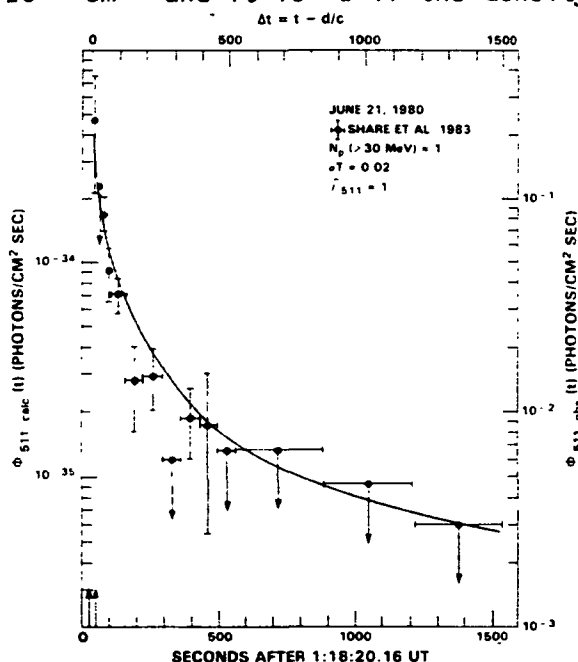


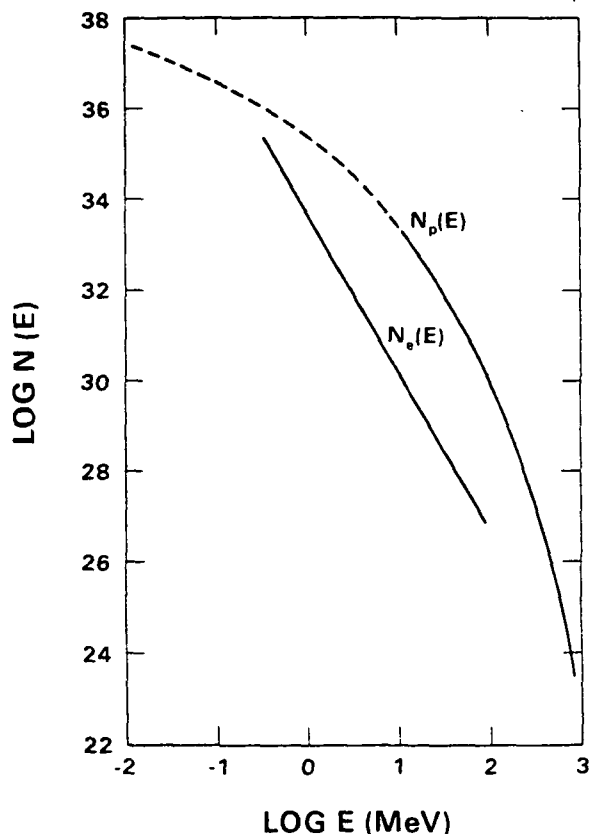
Fig. 4. Observed and calculated 0.511 MeV line flux at Earth.

The curve in Figure 4 shows the calculated time-dependent 0.511 MeV line flux at Earth from a burst of positron-emitter production at  $t = 0$  for thick-target interactions, photospheric abundances,  $\alpha T = 0.02$ , negligible positron slowing-down and annihilation times and  $\bar{f}_{0.511} = 1$ . Also shown in this figure is the 0.511 MeV line flux observed from the June 21, 1980 flare<sup>30</sup>. As for the neutron production, we assumed that the positron-emitter production time was at 1:18:55 UT-d/c, i.e. at the midpoint between the two impulsive photon emission

peaks shown by arrows. As can be seen, the shape of the observed time dependence fits the calculations quite well. The fact that the lag, if any, between the observations and calculations is less than about 10 sec, implies that the density in the annihilation site should exceed about  $2 \times 10^{11} \text{ cm}^{-3}$ . For  $\bar{f}_{0.511} = 1$ , the absolute normalization of the data to the calculations implies that  $N_p(>30 \text{ MeV}) \sim 5 \times 10^{32}$ , in good agreement with the value of  $N_p(>30 \text{ MeV}) \sim 1.2 \times 10^{33}$  obtained above from the high-energy neutron observations.

## CONTINUUM GAMMA-RAY EMISSION

Gamma-ray continuum in solar flares is produced by electron bremsstrahlung and  $\pi^0$  meson decay. We first consider the production of bremsstrahlung in the thick-target model.



Using calculations of bremsstrahlung emission<sup>33</sup> and the electron energy loss<sup>20</sup> in a neutral medium, we find that the time-integrated photon production is  $Q(\epsilon) \approx KF(s)\epsilon^{-s+\Delta s}$  photons/MeV, where  $N_e(E) = KE^{-s}$  electrons/MeV is the number of accelerated electrons incident on the interaction region,  $E$  and  $\epsilon$  are, respectively, the electron and photon energies in MeV,  $F(s) \approx 0.15 \exp(-s/0.55)$  and  $\Delta s \approx 1.2$ . These approximate formulae are valid for  $E$  and  $\epsilon$  between about 0.3 and 30 MeV, for  $s$  between about 3 and 4, and for an isotropic electron distribution in the interaction region. The observed<sup>4</sup> gamma-ray continuum from the June 21, 1980 flare in the energy

Fig. 5. Energy spectra of protons and electrons accelerated in the June 21, 1980 flare.

range from about 0.3 to 1.0 MeV was about  $730 \epsilon^{-2.3}$  photons/cm<sup>2</sup>/MeV. This implies that  $N_e(E) \approx 8 \times 10^{33} E^{-3.5}$  electrons/MeV. If synchrotron losses in the interaction region were also important,  $s$  would have to be less than 3.5.

At photon energies  $>1$  MeV, in addition to bremsstrahlung, nuclear radiation also make an important contribution to the solar flare gamma-ray continuum. In the energy range from 1 to 2 MeV, this contribution is<sup>34</sup> mainly from Mg, Si and Fe, and in the 4 to 7 MeV range, as discussed above, it is mostly from C, N and O. At energies  $>10$  MeV radiation from  $\pi$  mesons could contribute to the observed emission, but calculations<sup>11</sup> indicate that for the June 21, 1980 flare this contribution is quite small. Specifically, we find that the photon fluences above 10 MeV from  $\pi$  mesons from this flare, 0.07 and 0.35 photons cm<sup>-2</sup> for  $\alpha T = 0.02$  and  $s = 5.5$  respectively,

are much smaller than the observed (D. Forrest, private communication 1982) fluence of 30 photons/cm<sup>2</sup>.

The >10MeV emission seen from the June 21, 1980 flare, therefore, is most probably bremsstrahlung of directly-accelerated electrons. Indeed, the extrapolation of the observed<sup>4</sup> fluence between 0.3 to 1.0 MeV to energies >10MeV, giving a fluence of ~ 28 photons/cm<sup>2</sup>, can account for the observations. This implies that the electron distribution  $N_e \approx 8 \times 10^{33} E^{-3.5}$ , deduced for energies between 0.3 and 1 MeV, continues without a significant spectral break up to at least 30 MeV. This result is consistent with the observed<sup>35</sup> interplanetary relativistic electron spectrum from the June 21, 1980 flare. Thus, synchrotron losses in the interaction region appear to be negligible in comparison with the ionization and bremsstrahlung losses at least up to 30MeV. This sets a lower limit on the density in the interaction region,  $n(\text{cm}^{-3}) > 1.4 \times 10^{12} (B_{\perp}/300 \text{ gauss})^2$ , where  $B_{\perp}$  is the perpendicular component of the magnetic field, typically<sup>1</sup> of the order of a few hundred gauss.

The above electron distribution, together with the proton distribution for the June 21, 1980 flare given by the Bessel function with  $\alpha T = 0.02$ , are shown in Figure 5. As can be seen, at energies above ~ 1 MeV the proton-to-electron ratio is quite large, a result generally consistent with Fermi acceleration<sup>20,21</sup>. The total energy content in the protons and nuclei implied by this spectrum is  $W \approx 2.4 \times 10^{30}$  erg, with 75% of this energy residing in particles >1 MeV. The energy content in electrons of energies greater than 0.3 MeV is only  $2.9 \times 10^{28}$  erg, but more energy resides in the lower energy particles.

#### SUMMARY AND CONCLUSIONS

We have reviewed the theory of gamma-ray and neutron production in solar flares. We have discussed the production of neutrons, the attenuation of the 2.223 MeV line by Compton scattering in the photosphere, the production of a variety of observable nuclear deexcitation lines, methods for determining the number and energy-spectrum of the charged particles accelerated in flares, the production of positrons and the time dependence of the 0.511 MeV line, and continuum gamma-ray production by thick-target bremsstrahlung.

The time dependence of the high-energy neutron flux from impulsive flares determines<sup>11,19</sup> the energy spectrum of the accelerated protons in the energy range from about 10<sup>2</sup> to 10<sup>3</sup> MeV. For the June 21, 1980 flare this spectrum can be fit equally well by a power law with spectral index  $s=5.5$  or by the Bessel function appropriate for stochastic Fermi acceleration<sup>20,21</sup> with  $\alpha T=0.02$ . These and all other spectral parameters discussed here pertain to the particles that emerge from the acceleration region and are incident on the thick-target interaction region.

The ratio of the 4-7MeV-to-2.223MeV fluences from flares determines<sup>1</sup> the energy spectrum of the protons and nuclei in the 10 to 10<sup>2</sup> MeV/nucleon range. Analysis of data from several disk flares

implies that the particle spectrum in this energy range does not vary much from flare to flare, the values of the parameters  $s$  and  $\alpha T$  being about 3.5 and 0.02, respectively. By comparing these results with those obtained from the high-energy neutrons, it follows that over the entire 10 to  $10^3$  MeV range the proton spectrum cannot be fit by a single power law. The Bessel function, on the other hand does provide an acceptable fit. A similar conclusion is also obtained from interplanetary proton observations<sup>29</sup>.

The proton spectrum in the  $10^2$  to  $10^3$  MeV range, deduced from the neutron observations, is too steep to produce enough  $\pi$  mesons to account for the gamma-ray observations at energies  $>10$  MeV. Radiation at these energies from flares is therefore mostly electron bremsstrahlung<sup>11,19</sup>. In the energy range from 0.3 to 30 MeV, the implied electron spectrum for the June 21, 1980 flare is a power law with spectral index  $s \approx 3.5$  and the electron-to-proton ratio is energy dependent and much less than 1. This electron spectral index is similar to the index of the relativistic electrons observed<sup>35</sup> in interplanetary space from this flare.

The proton and relativistic electron acceleration mechanism in solar flares that has so far been studied in greatest detail is stochastic Fermi acceleration<sup>20,21,36</sup>. The particle spectra that result from this mechanism are consistent with the observed or inferred spectra provided that turbulence capable of scattering and accelerating both the protons and electrons exists in the acceleration region. Specifically, a shorter scattering mean free path is required to accelerate the electrons than the protons. Given that the necessary turbulence exists, stochastic acceleration is fast enough<sup>21,36</sup> to account for the short acceleration time implied<sup>4,37,38</sup> by the gamma-ray observations. But it remains to be shown whether the turbulence can develop fast enough.

The neutron and gamma-ray observations provide meaningful information on the interaction site of the accelerated particles. An upper limit on the density of the ambient medium at this site is set by the observation of high-energy neutrons from a limb flare. These observations imply<sup>19</sup> that the accelerated particles are stopped at densities  $<5 \times 10^{15} \text{ cm}^{-3}$ , essentially at the top of the photosphere, probably by magnetic mirroring<sup>24</sup> or scattering by magnetic irregularities. Lower limits on this density are set by the time dependence of the 0.511 MeV line flux and by the upper limit on the synchrotron loss rate of relativistic electrons ( $< 30$  MeV) in the interaction region. These limits are  $n_H > 2 \times 10^{11} \text{ cm}^{-3}$  and  $n_H (\text{cm}^{-3}) > 1.4 \times 10^{12} (B/300 \text{ gauss})^2$ , respectively. Since  $B$  is expected to be at least 300 gauss, the density should exceed about  $10^{12} \text{ cm}^{-3}$ . The interaction site, therefore, is the chromosphere.

#### REFERENCES

1. Chupp, E. L. et al. 1973, *Nature*, **241**, 333.
2. Hudson, H. S. et al. 1980, *Ap. J. (Letters)*, **236**, L91.
3. Chupp, E. L. et al. 1981, *Ap. J. (Letters)*, **244**, L171.

4. Chupp, E. L. 1982, in R. E. Lingenfelter et al. (eds.) Gamma-Ray Transients and Related Astrophysical Phenomena, AIP, N.Y., p. 363.
5. Forrest, D. J. 1983, in M. L. Burns et al. (eds.) Positron-Electron Pairs in Astrophysics, AIP, N.Y., p.3.
6. Prince, T. A. et al. 1982, Ap. J. (Letters), 255, L81.
7. Yoshimori, M. Okudaira, K., Hirasima, Y. and Kondo, I., 1983, Solar Physics, 86, 375.
8. Chupp, E. L. et al. 1982, Ap. J. (Letters), 263, L95.
9. Chupp, E. L. et al. 1983, 18th International Cosmic Ray Conference Papers, in press.
10. Evenson, P., Meyer, P. and Pyle, K. R. 1983, Ap. J. in press.
11. Ramaty, R., Murphy, R. J., Kozlovsky, B. and Lingenfelter, R. E. 1983, Solar Physics, 86, 395.
12. Von Rosenvinge, T. T., Ramaty, R., and Reames, D. V. 1981, 17th Internat. Cosmic Ray Conference Papers, Paris, 3, 28.
13. Ramaty, R., Lingenfelter, R. E., and Kozlovsky, B. 1982, in R. E. Lingenfelter et al. (eds.) Gamma-Ray Transients and Related Astrophysical Phenomena, AIP, New York, p. 211.
14. Lingenfelter, R. E. and Ramaty, R. 1967, in B. S. P. Shen (ed.), High Energy Nuclear Reactions in Astrophysics, W. A. Benjamin, New York, p. 99.
15. Wang, H. T., and Ramaty, R. 1974, Solar Phys., 36, 129.
16. Prince, T. A. et al. 1983, 18th International Cosmic Ray Conference Papers, 4, 79.
17. Chupp, E. L. 1983, Solar Physics, 86, 383.
18. Lingenfelter, R. E., Flamm, E. J., Canfield, E. H., and Kellman, S. 1965, J. Geophys. Res., 70, 4077, 4087.
19. Ramaty, R., Murphy, R. J., Kozlovsky, B. and Lingenfelter, R. E. 1983, Ap. J. (Letters) 273, L41.
20. Ramaty, R. 1979, in J. Arons et al. (eds.) Particle Acceleration Mechanisms in Astrophysics, AIP, New York, p. 135.
21. Forman, M. A., Ramaty, R. and Zweibel, E. G. 1983, in P. A. Sturrock et al. (eds.), The Physics of the Sun, in press.
22. Ramaty, R. 1984, in P. A. Sturrock et al. (eds.), The Physics of the Sun, in press.
23. Vernazza, J. E., Avrett, E. H., and Loeser, R. 1981, Ap. J. Suppl., 45, 635.
24. Zweibel, E. G. and Haber, D. 1983, Ap. J., 264, 648.
25. Ramaty, R., Kozlovsky, B., and Lingenfelter, R. E. 1979, Ap. J. Suppl., 40, 487.
26. Kozlovsky, B. and Ramaty, R. 1974, Ap. J. (Letters), 191, L43.
27. Ramaty, R., Kozlovsky, B., and Suri, A. N. 1977, Ap. J., 214, 617.
28. Ibragimov, I. A. and Kocharov, G. E. 1977, Sov. Astron. Lett., 3 (5), 221.
29. McGuire, R. E., Von Rosenvinge, T. T., and McDonald, F. B. 1981, 17th Internat. Cosmic Ray Conference Papers, 3, 65.

30. Share, G. H., Chupp, E. L., Forrest, D. J. and Rieger, E. 1983, in M. L. Burns et al. (eds.), Positron-Electron Pairs in Astrophysics, AIP, N.Y., p. 15.
31. Crannell, C. J., Joyce, G., Ramaty, R. and Werntz, C. 1976, Ap. J., 210, 582.
32. Bussard, R.W., Ramaty, R. and Drachman, R.J. 1979, Ap.J., 228, 928.
33. Bai, T. 1977, Studies of Solar Hard X-Rays and Gamma Rays: Compton Backscatter, Anisotropy, Polarization and Evidence for Two Phases of Acceleration, Ph.D. Dissertation, University of Maryland.
34. Ramaty et al. 1980, in P. A. Sturrock (ed.) Solar Flares, Colorado Assoc. Univ. Press, Boulder, p. 117.
35. Evenson, P. et al., 1984, preprint.
36. Melrose, D. B. 1984, Solar Physics, in press.
37. Bai, T.: 1982, in R. E. Lingenfelter et al. (eds.) Gamma-Ray Transients and Related Astrophysical Phenomena, AIP, N.Y., p. 409.
38. Forrest, D. J. and Chupp, E. L. 1983, Nature, 305, 291.

## GAMMA RAY BURSTS: A 1983 OVERVIEW

T. L. Cline  
 NASA/Goddard Space Flight Center, Greenbelt, MD 20771

## ABSTRACT

Gamma-ray burst observations are reviewed with mention of new gamma-ray and optical transient measurements and with discussions of the controversial, contradictory and unresolved issues that have recently emerged: burst spectra appear to fluctuate in time as rapidly as they are measured, implying that any one spectrum may be incorrect; energy spectra can be obligingly fitted to practically any desired shape, implying, in effect, that no objective spectral resolution exists at all; burst fluxes and temporal quantities, including the total event energy, are characterized very differently with differing instruments, implying that even elementary knowledge of their properties is instrumentally subjective; finally, the  $\log S$  - $\log S$  determinations are deficient in the weak bursts, while there is no detection of a source direction anisotropy, implying that Ptolemy was right or that burst source distance estimates are basically guesswork. These issues may remain unsolved until vastly improved instruments are flown.

## INTRODUCTION

A new stage has been reached in the history of gamma-ray burst studies, in my opinion. The first decade since their discovery<sup>1</sup> closed with a several-year period rich in observations and discoveries and accompanied by optimism generating theoretical ideas that are still undergoing development. Now, however, more detailed analyses of the experimental results as a whole appear to have produced a contrasting scenario, characterized by contradictions, confusion and overall lack of definition. Also, the density of additional, recent discoveries has diminished and includes few new surprises, with the one remarkable exception of that of archived optical flashes in gamma-ray burst source fields<sup>2,3</sup>.

Reviews I have recently given<sup>4,5,6</sup>, which I will try not to repeat here, covered those exciting experimental developments with which we are now familiar: these include the detection and detailed study of the 1979 March 5 transient with its unusual properties<sup>7,8,9</sup> and its source field in the location of the supernova remnant N49 in the LMC<sup>10,11,12</sup>; the precise source positions of other gamma-ray bursts that, in contrast, have no optical source counterparts that can be identified<sup>13,14,15,16</sup>; the spectral features of bursts that are interpreted at low energies to be cyclotron resonant features and at higher energies to include redshifted annihilation and other lines<sup>17,18,19,20</sup>; the detection of repeated mini-events from two specific source areas, one of which is the same as that of the 79 March 5 event<sup>21,22</sup>; the lack, with one possible exception<sup>23,24</sup> of X-ray counterparts and of radio counterparts<sup>25</sup> of burst sources; and

---

Invited paper, presented at the University of California, Santa Cruz Summer Workshop on "High Energy Transients", July 1983 to be published in AIP Conference Proceedings, 1984.

the 1928 archived optical transient recently associated with a 1978 burst<sup>2</sup>. This review immediately follows the review by Kevin Hurley<sup>26</sup>, who also produced other recent reviews that should be referenced<sup>27,28,29</sup>. In addition, there is a review specializing on spectral observations, given by Bonnard Teegarden<sup>30</sup> later in this conference. Also, there will be a variety of theoretical treatments here, including those that champion specific interpretations. I seem to be left with very little to do; however, I feel it is a necessary task to present my view of the present state of the observations--the impossibility of unambiguous experimental interpretation and the attendant overall state of ignorance--to provide a certain kick-off flavor for this Conference. Further, given the natures of all the instruments either in use or under development for future measurements (with the notable exceptions of GRO and RMT), this situation may not soon be entirely alleviated. Recognition of the need to design a specific, next-generation experiment array that may solve this basic scientific problem, in fact, is one of the common goals bringing us here now.

#### NEW RESULTS ON THE 1979 MARCH 5 EVENT

In some areas of endeavor, there have recently been produced new experimental results; one of these is that related to the 1979 March 5 event. My earlier review of these phenomena<sup>5</sup> is no longer complete; data collected on that event have been reanalyzed and newer observations also pertain. Hurley's review<sup>26</sup> outlines evidence for the  $\approx 40 \text{ second}^{-1}$  frequency of intensity decreases in the 150-millisecond-wide intensity peak (contrasting with the well-known 8-second decay period and implying reinterpretations of either rotational, torsional, precessional or plasma oscillations) seen in the Moscow-Toulouse data<sup>31</sup>. He also mentions Leningrad observations of continuing mini-event activity from the source direction of this event<sup>32</sup>. What can be added for completeness in this brief review is elaboration on the curious shape of one of these events. Figure 1a illustrates the evidence for source commonality.

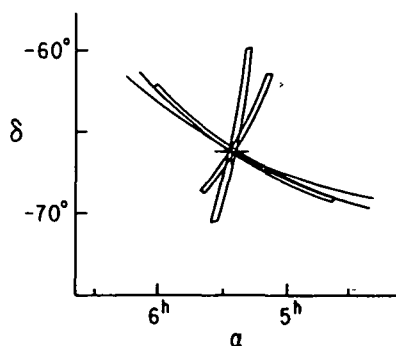


Figure 1a. Source loci of several of the recurrent transients recently found by Mazets and coworkers<sup>32</sup> to occur randomly in 1981-2, as well as days to weeks after the March 5 event in 1979. The cross marks the most precise location of that event<sup>12</sup>.

The figure shows that the several source positions are each compatible with that for the 1979 March 5 event, and, together, independently reinforce a pattern that overlaps giving a region that agrees with that position. This is a critical issue, since theoretical models exist that can support an N49, or 55-kpc distant, source. The curious shape of the 1981 December 1 event is what is new here; unlike the others of the series, it is essentially a square wave, as shown in Figure 1b. The 1979 March 5 event decay possessed a periodic 8-second compound shape, tracked for over 3 minutes<sup>8</sup>, yet this burst, from the same source, is sufficiently extended in time, unlike the other very brief bursts in the mini-series, to show absolutely no evidence for this effect. This phenomenon is a new puzzle for theoreticians' ingenuity.

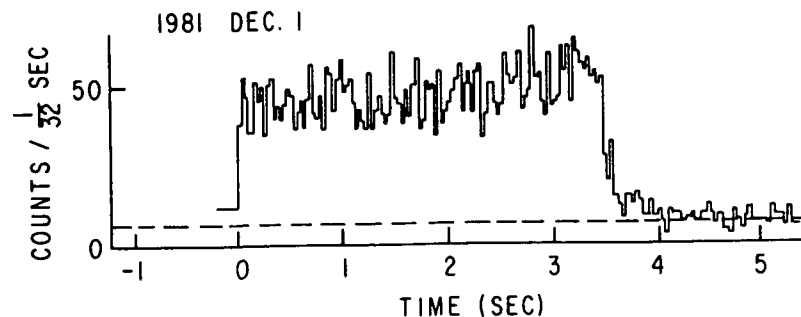


Figure 1b. The longest-duration mini-event in the series from the source of the 1979 March 5 event: a remarkable square wave.

Other new results on the 1979 March 5 event are reprocessed old data. One is the verification of the well-known uniqueness of its time history, as mentioned in Hurley's review<sup>26</sup>. (All other single-spike time-history gamma-ray bursts fit into one continuous population when plotted on a rise-time versus decay-time scatter diagram; the March 5 event is not unusually brief in duration but remains unique in its fast rise time.) Finally, the Franco-Soviet data have been scrutinized to reveal one interesting effect in the spectral evolution. Figure 2a shows the differential spectrum of the initial 24 milliseconds, with a peak near the 400-keV region; figure 2b shows the following-one-quarter-second spectrum possessing no evidence for such a feature<sup>33</sup>. Two concerns immediately surface: first, one can question whether the 420-keV peak in the event-integrated spectrum of this burst, usually attributed to a red-shifted annihilation line, is a phenomenon of the 24 ms onset only, or is it merely an artifact of summing two continuum spectra? Second, what would this event look like--whichever is the case--if significantly faster spectral resolution could have been available?

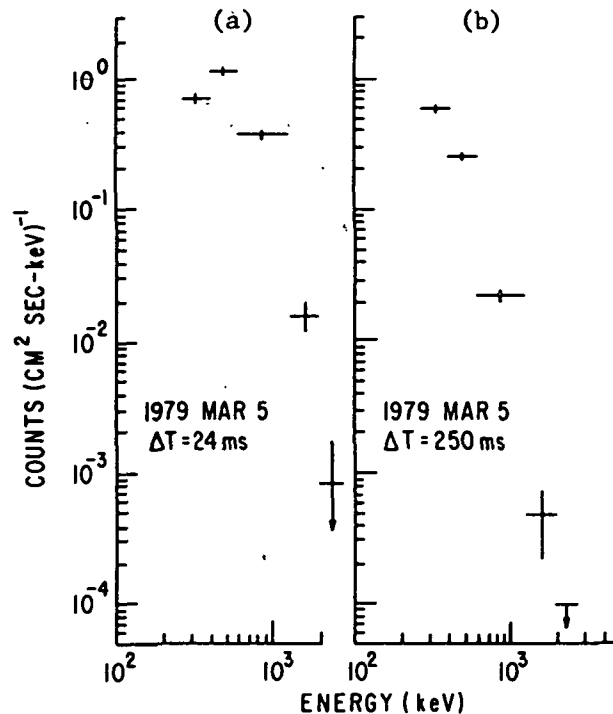


Figure 2. Recently extracted measurements of the spectra<sup>33</sup> of the 1979 March 5 event, showing an intensity peak consistent with the 420 keV feature, dominating for the initial several tens of milliseconds. The resolution of this detector does not permit discriminating between a pure, redshifted annihilation line and a broad continuum with a maximum at the same energy, although one suspects that the pure line should be accompanied by a lower-energy continuum.

#### SPECTRAL AND TIME-HISTORY CONSIDERATIONS

The above concerns as to the true nature of the spectrum of the 1979 March 5 event introduce and emphasize a more general problem: are we being fooled as to the natures of all burst spectra? Several independent, new analyses of typical bursts, using data from different instruments on differing spacecraft, indicate that their spectra change dramatically in time as rapidly as they are measured<sup>34,35</sup>, just as illustrated above for the March 5 event. If this can be so, then it is immediately apparent that burst spectra could fluctuate yet more rapidly. An old measurement of ours showed, nearly a decade ago, that typical, large bursts usually have the same event-integrated burst spectrum<sup>36</sup>: yet, as we have known for some years, spectra fluctuate within their event durations. Thus, it is perfectly possible also not only that they may change faster than are monitored but that similar

spectra taken within a given event at different times, that mutually agree and thus appear to be reliable, may also be composed of finer time structures that each differ in detail. In summation, it seems fair to claim that we have good reason to believe that we may have little or no knowledge of an instantaneous gamma-ray burst spectrum. Given this fact, any deductions drawn from the appearance of burst spectra may be quite fallacious.

Other facts to be given attention at this Conference include the 'impure' and 'obliging' natures of the spectra. The aspect of the (usually) disk-shaped detector, relative to the source direction, and the directional scattering qualities of the spacecraft are of significance, yet may be unknown or at least poorly defined. Also, it is not always appreciated, by those who do not build low-energy gamma-ray detection instrumentation at least, that gamma-ray spectra in this most pernicious energy domain are actually not uniquely defined although obtained using perfectly operating equipment. The unfolding of the spectrum of secondary electrons amplified in the sensing apparatus depends on the assumed spectrum of incident gamma-rays: differing input distributions produce lower-energy secondaries in manners that, taken together with the energy-dependent detection efficiencies, can give similar results, 'obligingly'. The actual spectral source form is therefore not only not necessarily calculable, but can be linked to (or not independent of) the resulting spectral fit a particular researcher wants to investigate. Hence, and for another reason, gamma-ray burst spectra are presently 'unresolved'.

Time histories of a given event, taken with different instruments, vary dramatically, as is well known. This then can be appreciated if one recognizes that the observed counts above a given energy threshold are integrated in each detector, so as to provide optimum count rate statistics, and different detectors not only have differing thresholds but are quite unlike in their efficiency profiles as a function of energy. What compounds this situation, however, as is implied by the previous discussion, is the inability to deduce a unique input photon energy spectrum from the output count rate distribution. Hence the astounding lack of agreement (even to discrepancies approaching two orders of magnitude<sup>37</sup>) regarding the total energy quantity in a given event. If any one event cannot be well characterized as to its size, how then can a meaningful size spectrum be deduced?

#### GAMMA-RAY BURST SIZE SPECTRUM

The compilation of measurements of integrated number of burst events as a function of total energy, the so-called  $\log N (>S) - \log S$  plot, that is most often quoted as shown in Figure 3. This figure, from Jennings<sup>38</sup>, is fairly recent but does not include additional, weak-flux upper limits from HEAO-1 X-ray data<sup>39</sup> and a balloon flight of the Gamma Ray Observatory prototype<sup>40</sup> reported at this Conference. These indicate a dramatic flattening of the experimental point scatter, that is, an even greater departure from the -1.5 index power-law shape expected from an indefinitely extended, isotropic source spatial distribution.

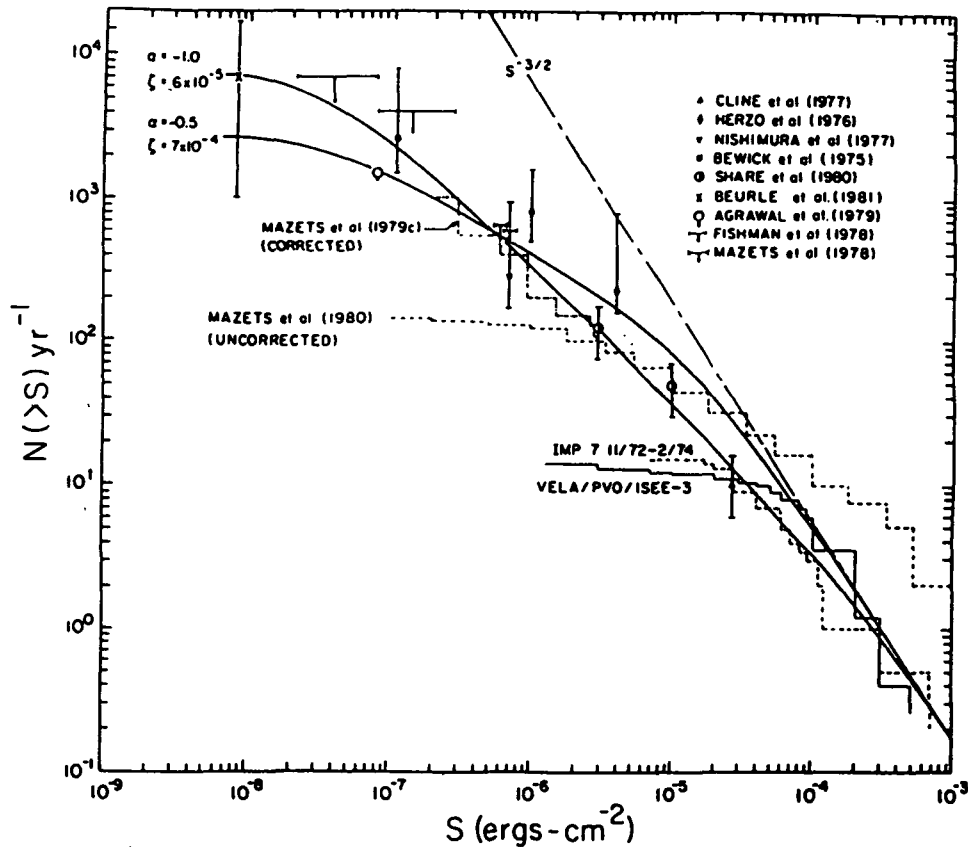


Figure 3. The often-quoted log N-log S plot of burst sizes, expressed in terms of total energy per event<sup>38</sup>.

Fishman's results<sup>40</sup> with a GRO prototype are particularly tantalizing: the use of an instrument with total collecting area between one and two orders of magnitude larger than any of those on the Venera or other spacecraft yielded one event in several days continuous operation. Even taking into account terrestrial and atmospheric shielding, this result provides the unquantified but distinct qualitative impression that there are hardly any more weak events per unit time than have previously been counted with spacecraft. A flattening in the integral spectrum, however, is not possible in a galactic disk model if there is no event anisotropy for those same events. Admittedly, only the directions of the more intense can be well determined, but the directions of all the weakest, as monitored with the Leningrad experiments on the Veneras, are adequately determined so as to investigate the questions of the existence of an anisotropy of source patterns: note that the mini-series following the 1979 March 5 event, although weak, are localizable to up to  $10^{\circ}$  accuracy in the worst dimension (Figure 1a). Further, note the existence of a control experiment: if Mazets' equipment can discern the presence of a mini-series from the LMC, it

could also see such a population from the galactic disk or center, which it does not. Thus, we have another puzzle: weak events, not including the separate mini-series, are lacking in number and yet are essentially isotropic. It could be argued that there are not enough to statistically establish the presence of an anisotropy, but that is precisely part of the same problem: they are not there, but they should be present in greater numbers than the stronger events if the strong events come from nearby sources--unless the source distribution breaks into a galactic disk component, in which case the number should still increase by the -1 index power law and exhibit a disk anisotropy, which is not observed.

I do not believe that there exists a spherically symmetric nearby component of burst sources, arranged only around the solar system, obeying the ptolemaic model. Jennings<sup>38</sup> gets around this problem with a galactic halo model; that idea may require emission mechanisms even more difficult to treat theoretically than having the source of the 1979 March 5 event in N49 at 55 kpc--since then even ordinary bursts have their source distances at essentially that same value. Another way out is to invoke peak event flux, rather than total event energy, as the relevant size characteristic. One can also consider a reevaluation of the various assumptions concerning the instrument capabilities to give more realistic estimates of measurement limitations<sup>41</sup>. These approaches each operate in the direction so as to shrink and straighten the size spectrum: we are left, however, with no remaining knowledge or implications as to burst source distances.

#### SOURCE POSITIONS AND OPTICAL TRANSIENT ASSOCIATIONS

The one ray of hope in this picture, given the present situation of no next-generation instruments going soon into orbit, is the implication of Schaefer's discovery of archived optical transients in burst source fields<sup>2</sup>. Figure 4 shows the first transient located within the 1978 November 19 burst<sup>13</sup> source error box. Since optical transients are resolved with several seconds of arc positional accuracy, whereas burst directions can be resolved to only a fraction of an arc minute, one to two orders of magnitude improvement is achieved in providing source object search areas. Further, an additional dimension of investigating source properties is provided in this new wavelength domain. To date,<sup>3</sup> three convincing optical transient-burst associations have been found, the second and third of which come from precisely determined but as yet unpublished interplanetary network source observations. More of these small error boxes are still in production from the first network, while the necessary orbital data are not yet available to analyze the bursts recently observed with the second network, incorporating Veneras-13 and -14. Yet another network will be created when ISEE-3 departs the Earth's environment for its comet encounter; further, Solar Polar is yet to be launched. Thus, we can expect a continuing production of precise error boxes to be forthcoming during the next few years. Scrutiny of all these in photographic archives may yield additional optical transients; in my opinion, the three are enough to establish the validity of this association.

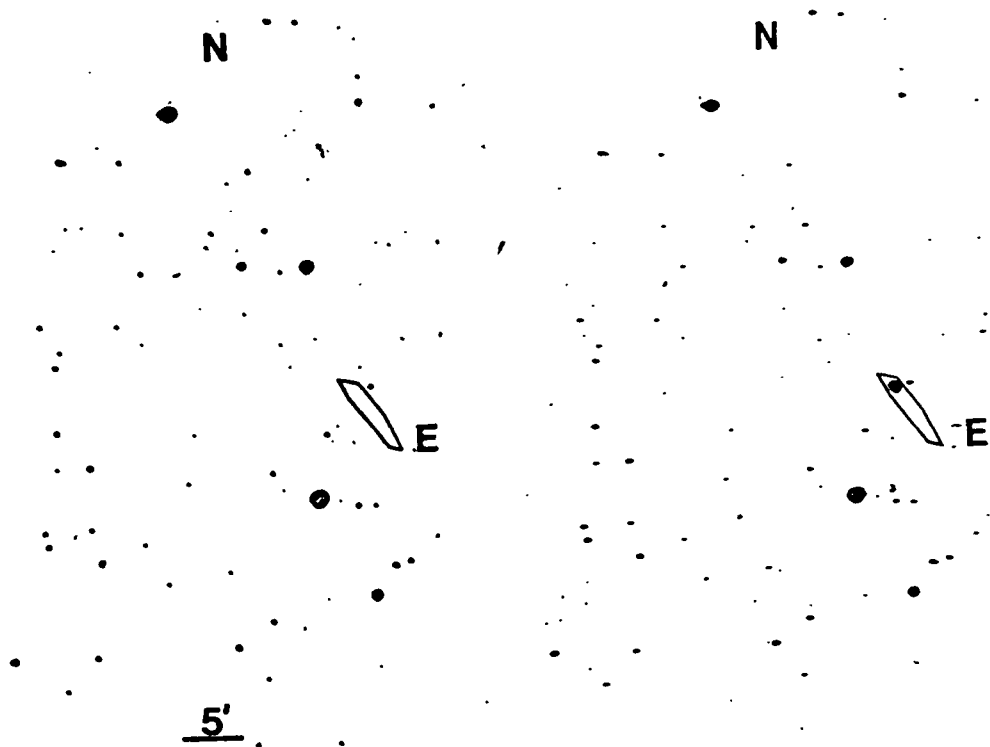
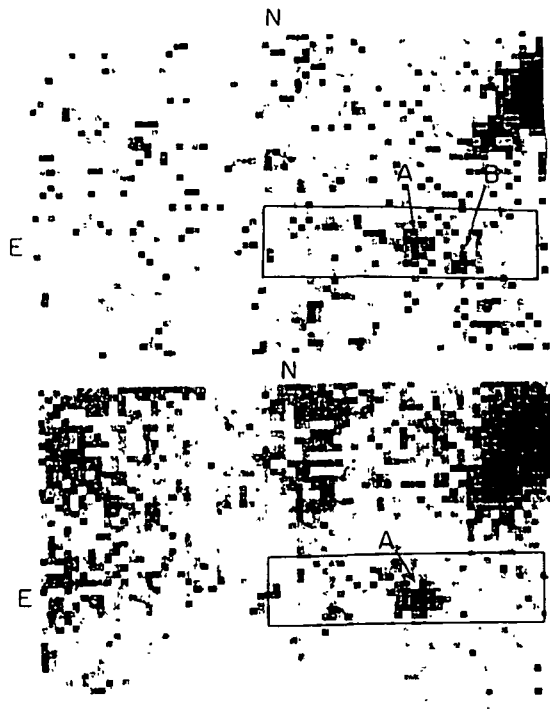
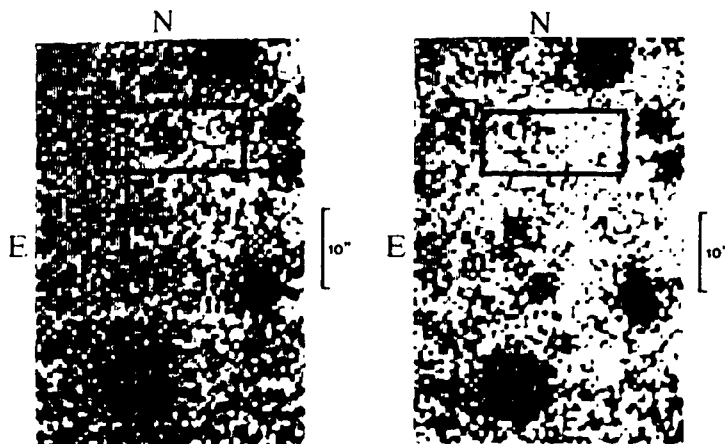


Figure 4a and 4b. The 1928 optical transient<sup>2</sup> in the 1978 November 19 burst source field<sup>13</sup>. Reducing the error field by an order of magnitude<sup>6</sup> will include the optical transient position.

This very small optical source area has been further scrutinized with deep optical searches in the present epoch<sup>42,43</sup>. These results are shown in Figures 5 and 6. No steady identifiable source object exists in this region down to  $\approx 22^{\text{nd}}$  magnitude. Many hours of collecting time with the most sensitive optical instruments in existence are needed in order to reveal limits of fainter objects. One set of results shows both one steady source and one variable (on during 1981 July to 1982 July and off during 1982 September to 1982 December)<sup>42</sup>. Each of these is in the 24th-magnitude ball park, depending on color considerations. Another set of observations confirms the absence of the off-source during the same time window, but shows that the one steady source actually varies by one magnitude or more on a time scale of under 1 day<sup>43</sup>. In addition, these observers find at least one additional fainter source of greater than 25th magnitude. As a result, one cannot claim that the candidate source object has been unambiguously identified. Complicating this situation, in addition, is the fact that the source object may not, in 1982, still be inside the 1928 source field: even at great distance, it could exhibit proper motion of up to one arc minute during a half-century and remain inside the 1978 burst error box. The true optical source field would contain one to two orders of magnitude more background objects.



Figures 5a and 5b. European Southern Observatory studies of the 1928 optical transient region, marked with a 4" x 16" sized error box<sup>43</sup>. One source appears to be steady (the two exposure times are not the same); the other has definitely turned off.



Figures 6a & 6b. Cerro Tololo Inter-American Observatory studies; the error region is marked here at  $\approx 6'' \times 16''$ . The brightest source is variable; its location is that of the steady source in Figure 5. Other weaker sources may exist; the candidate burst source object is therefore not unambiguously identified.

#### SUMMARY

I have presented a picture of the lack of definition of gamma-ray burst measurables: it is not a question merely of the degree of accuracy, but of the resolution that is inadequate to resolve, identify or define basic source and emission properties. The future use of optical transient monitors, as described by Ricker and his colleagues at MIT<sup>44</sup>, coupled with the Rapidly Moving Telescope (RMT) of Teegarden and others at Goddard, may locate optical burst sources in real time that are simultaneous with gamma ray burst sources. Other, yet undefined, experimental efforts also will be necessary to solve these problems.

ACKNOWLEDGEMENTS: I have enjoyed recent conversations with many persons, especially U. Desai, E. Fenimore, K. Hurley, M. Jennings, R. Klebesadel, E. P. Mazets, J. Norris, B. Schaefer, and B. Teegarden. I thank J. Newby for her patient assistance with the manuscript.

## REFERENCES

1. R. W. Klebesadel et al., Ap. J. (Lett.) 182, L85 (1973).
2. B. E. Schaefer, Nature 294, 722 (1981).
3. B. E. Schaefer, Proceedings of this Conference.
4. T. L. Cline, Annals NY Acad. Sci. 375, 314 (1981).
5. T. L. Cline, A.I.P. Conference Proceedings 77, 82 (1982).
6. T. L. Cline, Adv. Space Res. 3, #4, 175 (1983).
7. E. P. Mazets et al., Nature 282, 587 (1979).
8. T. L. Cline et al., Ap. J. (Lett.) 237, L1 (1980).
9. T. L. Cline, Comments Ap. 9, 3 (1980).
10. W. D. Evans et al., I.A.U. Circular # 3356, May 11 (1979).
11. W. D. Evans et al., Ap. J. (Lett.) 237, L7 (1980).
12. T. L. Cline et al., Ap. J. (Lett.) 255, 245 (1982).
13. J. G. Laros et al., Ap. J. (Lett.) 245, L63 (1981).
14. T. L. Cline et al., Ap. J. (Lett.) 246, L133 (1981).
15. C. Barat et al., Ap. J., in print.
16. J. G. Laros; K. Hurley, private communication.
17. E. P. Mazets and S. V. Golenetskii, Ap. Space Sci. 75, 47 (1981).
18. B. J. Teegarden and T. L. Cline, Ap. J. (Lett.) 236, L67 (1980).
19. B. J. Teegarden and T. L. Cline, Ap. Space Sci. 75, 181 (1981).
20. E. P. Mazets et al., Nature 290, 379 (1981).
21. E. P. Mazets and S. V. Golenetskii, P.T.I. (Leningrad) Preprint 632 (1979).
22. S. V. Golenetskii et al., P.T.I. (Leningrad) Preprint 813 (1983).
23. G. Pizzichini et al., Space Sci Rev. 30, 467 (1981).
24. J. E. Grindlay et al., Nature 300, 730 (1982).
25. R. M. Hjellming and S. P. Ewald., Ap. J. (Lett.) 246, L137 (1981).
26. K. Hurley, Proceedings of this Conference.
27. K. Hurley, A.I.P. Conference Proceedings 77, 85 (1982).
28. K. Hurley, MPI Workshop Accreting Neutron Stars, Garching, (1982).
29. K. Hurley, Adv. Space Res. 3, #4, 163, (1983).
30. B. J. Teegarden, Proceedings of this Conference.
31. R. I. Hayles et al., COSPAR Proc., Rojen, Bulgaria, (1983).
32. E. P. Mazets, private communication.
33. K. Hurley, private communication.
34. C. Barat et al., COSPAR Proc., Rojen, Bulgaria (1983).
35. K. Hurley, private communication.
36. J. P. Norris, Univ. of MD, Ph.D. Thesis (1983).
37. R. W. Klebesadel, private communication.
38. M. C. Jennings, Ap. J. 258, 110 (1982).
39. A. Connors, private communication.
40. G. J. Fishman, private communication.
41. T. L. Cline and W. K. H. Schmidt, Nature 266, 749 (1977).
42. H. Pedersen et al., Ap. J. (Lett.) 270, L43 (1943).
43. B. E. Schaefer et al., Ap. J. (Lett.) 270, L49 (1983).
44. G. Ricker et al., Proceedings of this Conference.

THE SPECTRAL PROPERTIES OF GAMMA-RAY BURSTS:  
A REVIEW OF RECENT DEVELOPMENTS

B.J. Teegarden  
Goddard Space Flight Center, Greenbelt, MD 20771

ABSTRACT

Recent developments in the spectroscopy of gamma-ray bursts (GRB) are reviewed. The general question of the validity of the spectral results, particularly with regard to features in the spectrum, is discussed. Confirmations of these spectral features are summarized. Recent results from the KONUS experiments on Venera 13 and 14 are reviewed. The status of models of the continuum spectrum is summarized. A number of different radiation mechanisms appear capable of fitting the data. These include thermal brehmsstrahlung, thermal synchrotron and inverse Compton. Rapid variability of the spectral shape on time scales  $< 0.25$  sec. has been reported. The characteristic energy of the spectrum has been observed to vary over nearly an order of magnitude during individual events. A strong correlation between spectral hardness and luminosity has been found. Low-energy (50 keV) absorption features and high-energy (400 keV) emission features continue to appear in GRB spectra. Understanding the origin of these lines in the context of the existing continuum models remains a difficult problem.

INTRODUCTION

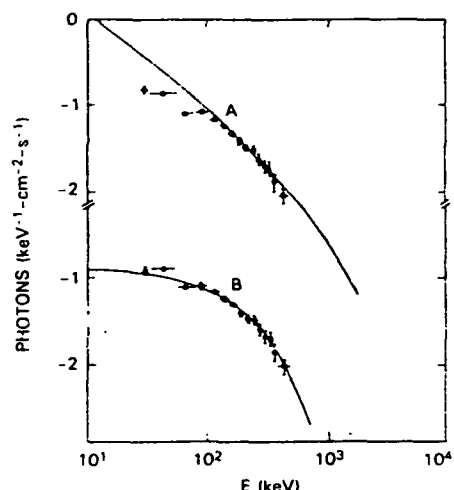
The study of the spectral behavior of gamma-ray bursts (GRB) has proven to be one of the most important avenues towards the understanding of the origin and mechanism of these events. Bursts are bright, energetic short-lived phenomena that are characterized by extremely hard spectra. Indeed the mechanism for producing such hard spectra is one of the most challenging of the many problems faced in modelling GRB's. Photons up to at least ten MeV have been observed in some events<sup>1</sup>, which puts severe constraints on the size of the emission region and the distance to the event. Rapid variability of the shape of the continuum spectrum has been observed on time scales  $< 0.2$  sec. (This is an instrumental limit and much faster variability may, in fact, exist.) Extensive modeling of the continuum spectrum has been performed<sup>2,3,4,5,6</sup>. At present the true nature of the emission mechanism remains an unsolved problem.

GRB's are known to display a wide variety of spectral features. Lines in the 30-80 keV region have been observed in  $\sim 30\%$  of GRB's<sup>7,8</sup> and are thought to be due to cyclotron absorption. Low-energy turn-overs have been reported, which may arise from a synchrotron cut-off or self-absorption<sup>6</sup>. Emission lines from red-shifted annihilation radiation ( $E \sim 400$  keV) are likely to exist<sup>7</sup>. Finally, there is some evidence for the presence of lines at higher energies which may be due to nuclear processes<sup>9</sup>. These data, taken together, give strong support to the hypothesis that GRB's originate on or near the surfaces of magnetized neutron stars.

This paper will concentrate on new results that have appeared during the past two years. For a treatment of previous results, the reader is referred to earlier reviews<sup>7,8,10</sup>.

### INTERPRETATION OF SPECTRAL DATA

The conversion of a raw detector or counts spectrum into a photon spectrum is a complex procedure which, in its most general form, involves a matrix multiplication. This is true since a photon



will, in general, not produce a unique signal in the detector, but will have a distributed spectrum of energy losses. Two effects are important: 1) A photon will not always deposit all of its energy in the detector. Some of the energy can escape due to K x-ray emission after photo-absorption or due to Compton scattering. 2) The energy resolution of the detector may be broad (i.e. greater than the bin width used in the data analysis). An iterative procedure is normally used wherein a model spectrum is assumed. This spectrum is multiplied by the

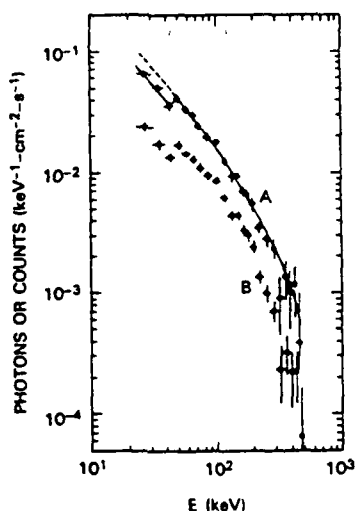
Fig. 1. Two different fits to the spectra of GB800419 (from Ref. 1). Curve A is an optically-thin thermal Brehmsstrahlung fit. Curve B is an exponential fit. Original data comes from the HXRBS experiment on SMM (see Ref. 12).

detector response matrix and the result compared with the raw spectrum. The parameters of the model spectrum are varied until a "best fit" is obtained (usually determined by a chi-squared test). A "photon" spectrum is usually given which is obtained by multiplying the raw spectrum by the ratio of the input model spectrum to the derived detector spectrum. The result is not necessarily unique, as there may well exist other models that fit as well or better than the one originally assumed.

The modelling and interpretation of GRB spectra is complicated by the effects described above. In particular, Fenimore<sup>3,11</sup> has questioned the validity of certain reported GRB spectral features. Fig. 1 is reproduced from Fenimore<sup>11</sup> and shows two different fits to the same spectral data obtained from the Hard X-Ray Burst Spectrometer (HXRBS) experiment on the Solar Maximum Mission (SMM)<sup>12</sup>. Curve A is a thermal brehmsstrahlung fit. The departure of the data points from this fit below 100 keV has been interpreted as a broad absorption feature<sup>12</sup>. Curve B illustrates an alternate possibility, an exponential fit. The points in the photon spectrum

will, in general, move when a different trial spectrum is used. The result, as is evident in curve B, is that an acceptable fit is produced over the entire energy range, and the "absorption" feature nearly disappears. In fairness it should be pointed out that this is a worst-case example since the energy resolution of the HXRBS instrument is poor relative to most other instruments that have measured GRB spectra. The data analysis is further complicated by the presence of a dead-layer in the CsI.

The preceding example points to the need for exercising extreme caution in the interpretation of spectral data, particularly with regard to the possible presence of features in the spectrum. The most extensive set of results in which evidence for such features exists is that of Mazets and co-workers<sup>7,8</sup> from the KONUS



experiments on the Venera 11-14 series of spacecraft. To what extent can these criticisms be fairly leveled at this data? First, it should be noted that narrow as well as broad spectral features appear in the KONUS data. An example of such a feature is given in Fig. 2. This figure is quite important in that it gives both the raw uncorrected "counts" spectrum as well as the derived "photon" spectrum. An absorption feature at  $E \sim 40$  keV is evident in both spectra. Qualitatively, these data make a much stronger case for the presence of an absorption feature than the data in Fig. 1. It should also be pointed out that the energy resolution and dead-layer problems of the SMM instrument are not

Fig. 2. KONUS spectra of the event GB820406b (from Ref. 8). Curve A is the derived photon spectrum, assuming a simplified TB input spectrum. Curve B is the raw counts spectrum from which A was derived. It has been shifted downward by a factor of two.

nearly as severe for the KONUS experiment. Second, the narrow absorption features are present in some events, absent in others and time-variable within individual events. This argues against an artifact of the instrument or the deconvolution procedure.

A recent measurement of a GRB spectrum from the HEAO A-4 experiment<sup>13</sup> (see Fig. 3) has provided an important confirmation of "cyclotron" lines. The instrument is a phoswich with a field-of-view of  $1.7^\circ \times 20^\circ$  FWHM in its lowest energy range and has a much lower background than the KONUS experiment. Furthermore, the spectral deconvolution is simplified by the Compton rejection of the phoswich, and the instrument has much finer energy-channel quantization than does KONUS. The clear presence of a cyclotron-like feature in the spectrum of this quite-different experiment

constitutes a very strong case for the validity of these features.

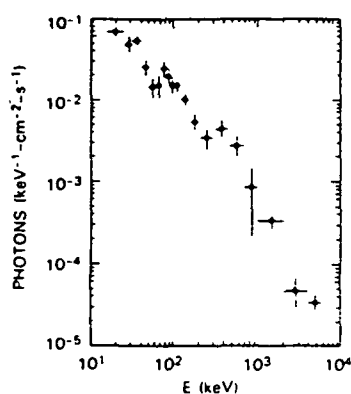


Fig. 3. HEAO A-4 spectrum of the event GB780325 (from Ref. 13). Evidence for an absorption line at 60 keV is clearly present.

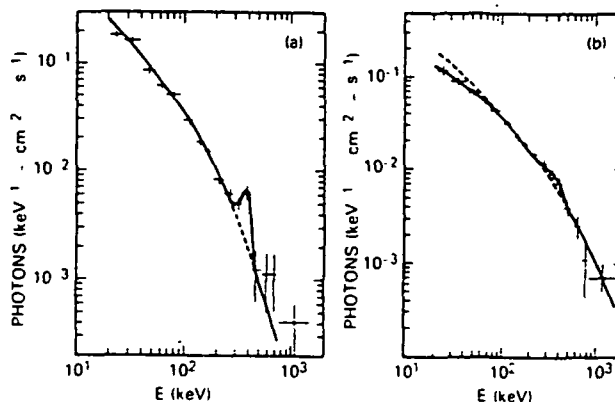


Fig. 4. Two examples of emission features at  $E \sim 400$  keV from the KONUS experiment. a) GB780918 (from Ref. 7). Solid curve is  $dN/dE \propto E^{-1} \exp(-E/185)$ . b) GB820320 (from Ref. 8). Solid curve is  $dN/dE \propto E^{-1} \exp(-E/640)$ .

Another type of spectral feature has been reported in the literature, again principally from the KONUS experiment<sup>7,8</sup>. This is a broad emission line ( $\Delta E \sim 200$  keV) with a centroid at  $E = 400$ - $500$  keV. It has been interpreted as red-shifted annihilation radiation originating near the surface of a neutron star (a gravitational red-shift of 15-20% is expected). In general these features are rarer in GRB spectra than the "cyclotron" lines. Such a feature is apparently present in Fig. 3 although not explicitly claimed in the original paper<sup>13</sup>. Two additional examples are given in Figs. 4a & b. The first of these, GB790918, displays a strong 400 keV line, whereas the second has a much weaker feature. Similar arguments to those raised for the "cyclotron" lines also apply here. Strong features are difficult to produce by instrumental artifacts whereas weak features could possibly disappear if a different input model spectrum is assumed.

A summary of the confirmations of the reported spectral features is given in Table I. These have been placed into two somewhat subjective categories "suggestive" and "probable". Generally speaking "suggestive" implies that the result was of marginal statistical validity or that some other instrumental difficulty exists. The Venera 13 and 14 results have been included even though the experiments are nearly identical to those that made the original discoveries. This is simply intended to point out that they are, in fact, finding essentially the same results as their predecessors. Table I indicates that the "cyclotron" features are on relatively firm ground whereas the "annihilation" lines are still in need of a solid confirmation. A third category of "other" is included that at present contains only one entry, the 740 keV line

reported by Teegarden and Cline<sup>9</sup>. No confirmation of this line exists at present, although the reader is referred to the paper by Matz in these proceedings for a very interesting and possibly relevant result.

TABLE I.  
CONFIRMATIONS OF GAMMA-RAY BURST SPECTRAL FEATURES

<u>Spectral Feature</u>	<u>Confirmation</u>	
	<u>Suggestive</u>	<u>Probable</u>
"Cyclotron" Lines		
Venera 13 & 14 <sup>8</sup>	-	x
Venera 13 & 14 <sup>19</sup>	-	x
HEAO 1 <sup>13</sup>	-	x
SMM <sup>12</sup>	x	-
"Annihilation" Lines		
Venera 13 & 14 <sup>8</sup>	x	-
Venera 13 & 14 <sup>19</sup>	x	-
ISEE-3 <sup>9</sup>	x	-
SMM <sup>1</sup>	x	-
Other		
ISEE-3 <sup>9</sup> (740 keV line)	-	-

#### GAMMA-RAY BURST CONTINUUM SPECTRA

The spectra of GRB's have been measured over the range from a few keV up to 10 MeV. The greatest body of spectral data is limited to the region from 20 keV to 1 MeV. Over this range the spectra generally display a characteristic exponential-like shape<sup>7,8</sup>. A number of different forms for the model spectrum have been tested and found to be consistent with the data. These are discussed in more detail in the following:

##### a) Thermal Bremsstrahlung

Historically thermal bremsstrahlung (TB) was the first model spectrum that was found to provide an acceptable fit to most of the data<sup>7,14</sup>. The non-relativistic form of this is given by:

$$\frac{dN}{dE} \propto \frac{g(E)}{E} \exp(-E/kT) \quad (1)$$

where  $g(E)$  is the Gaunt factor. (For  $kT > 100$  keV,  $g(E) \propto E^{-0.31}$ )<sup>15</sup>. Examples of TB fits to spectra from a GRB are given in Fig. 5<sup>8</sup>. This is a simplified form in which the Gaunt factor has been set equal to unity, which has the effect of somewhat raising the best-fit value of  $kT$ . Mazets and co-workers<sup>7</sup> have demonstrated that this form produces an acceptable fit for the great majority of GRB spectra.

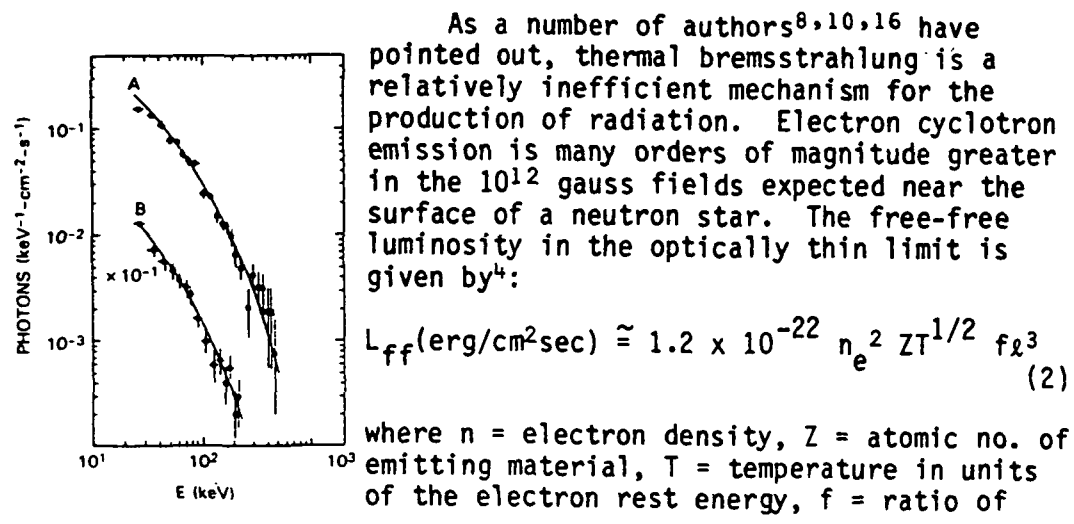


Fig. 5. KONUS spectra of the event GB820329 (from Ref. 8). Curve A is from the first 4 sec. of the event. Solid curve is  $dN/dE \propto E^{-1} \exp(-E/160)$ . Curve B is the third 4 sec. interval. Solid curve is  $dN/dE \propto E^{-1} \exp(-E/90)$ .

thickness to breadth of emitting region, and  $\ell$  = breadth of emitting region. If the region is optically thin then  $\tau = n_e \sigma f \ell < 1$  (where  $\sigma$  = electron scattering cross-section). The flux at the earth is given by  $F = L_{ff}/4\pi D^2$  where  $D$  is the distance to the source. Assuming a typical flux of  $10^{-6}$  erg/cm<sup>2</sup> sec. and combining these relations with equation 2 gives the following relationship:

$$\frac{f D^2(\text{pc})}{\ell(\text{km})} \lesssim 0.4 Z T^{1/2} \quad (3)$$

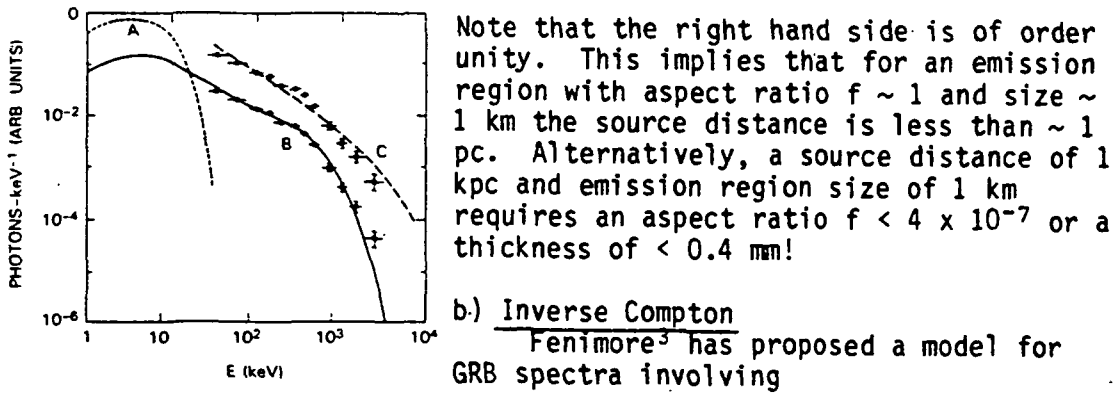


Fig. 6. IC fit to GB781104 (from Ref. 3). Curve A is the input 2.4 keV black-body spectrum. Curve B is the input spectrum Comptonized by a 155 keV electron gas. Curve C is a best-fit TB spectrum shown for comparison.

the inverse Comptonization (IC) of black-body photons by an overlying hot electron gas. Fig. 6 is an example of an inverse-Compton black-body fit to the first 4 sec. of the event GB781104. The best fit parameters are  $kT_{bb} = 2.4$  keV ( $T_{bb}$  = black-body temperature),  $kT_e = 155$  keV ( $T_e$  = temperature of hot overlying electron gas), and  $\rho x = 10^{24}$  e/cm<sup>2</sup>. Also shown for comparison is a TB fit to the same data. It is clear that, for this particular event, the inverse-Compton black-body provides a superior fit to the data. It should also be noted that here the TB model requires a very high temperature (3800 keV). The IC model has the attractive feature of being able to produce relatively hard spectra without requiring extremely hot plasmas. The departure from the TB fit at ~ 400 keV has been interpreted by Mazets et al.<sup>7</sup> as an "annihilation" line. This feature disappears when the IC spectrum is fit to the data. One of the difficulties with this model is the production and maintenance of the overlying hot electron layer. Strong magnetic fields (~ 10<sup>12</sup> gauss) have normally been invoked (see, e.g., Ref. 16) to confine the plasma long enough to produce the hot radiation in the burst. In this model, however, unless the field is less than ~ 10<sup>9</sup> gauss synchrotron emission will dominate.

### c) Thermal Synchrotron

Thermal synchrotron emission was first proposed by Ramaty et al. as an explanation for the continuum spectrum of the March 5 event. Liang<sup>4,5,6</sup> has developed in detail a model for GRB continuum spectra based on thermal synchrotron (TS) emission. He has found that, in

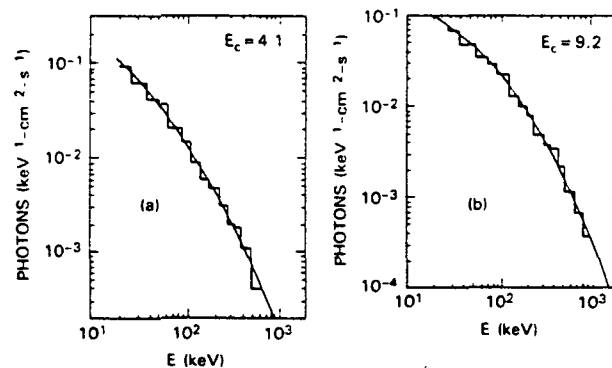


Fig. 7. Two examples of thermal synchrotron (TS) fits to GRB spectra (from Ref. 6). a) GB780930. b) GB790731. Original data is from KONUS.

the great majority of the KONUS events, the TS model provides an acceptable fit to the data<sup>6</sup>. Examples of such fits to two events are given in Figs. 7a & b. The form of the continuum spectrum for  $E \gg E_L$  ( $E_L$  = energy at Larmor frequency) is given by:

$$\frac{dN}{dE} \propto \exp \left[ - \left( \frac{4.5E}{E_c} \right)^{1/3} \right] \quad (4)$$

where  $E_c = E_L T^2 \langle \sin^2 \theta \rangle$ ,  $T$  = temperature in units of the electron

rest energy, and  $\theta$  = angle of the magnetic field with respect to the line-of-sight. Since  $E_L = ehB/mc = 11.6 B_{12}$  (KeV) we have that  $E_c \propto BT^2$ . Thus the shape of the continuum spectrum is not uniquely determined by the temperature, but depends on the strength of the magnetic field as well. Typical values for  $E_c$  lie in the 1-10 keV range<sup>6</sup>. If a value for  $B$  of  $2 \times 10^{12}$  gauss is assumed, this implies temperatures of 100-300 keV. Because of the quadratic dependence of  $E_c$  on  $T$ , the TS model can accommodate a wide range of GRB spectral shapes while requiring only a modest range in temperatures. The luminosity in the TS model is given by<sup>4</sup>:

$$L_{\text{syn}} = 2.7 \times 10^9 n_e VT^2 F(T) B_{12}^2 \text{ erg/sec} \quad (5)$$

where  $F(T) = 1/T$  for  $T \ll 1$ ;  $F(T) = T^2/K_2 (1/T)$  for  $T > 1$  ( $K_2$  = Bessel function). The TS model also predicts a variety of spectral features. Two examples are given in Figs. 8a & b. Fig. 8a shows a spectrum having a low energy turn-over. Two possibilities

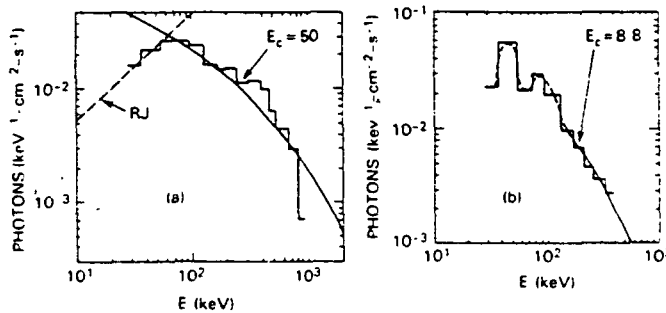


Fig. 8. a) KONUS spectrum of GB790402b with low-energy turn-over (from Ref. 6). Solid curve is TS fit to the high-energy portion of the spectrum. Dashed curve is  $E^2$  Rayleigh-Jeans form expected if synchrotron self-absorption is the cause of the turn-over. b) Spectrum of GB781012b with possible first and second harmonic emission lines.

exist: 1) In the TS model no emission will occur below  $E = E_L$ , the synchrotron cut-off. This would require placing  $E_L$  at  $\sim 70$  keV in this event. 2) The turnover could be due to synchrotron self-absorption. If this were true, then below the maximum the spectrum would assume a Rayleigh-Jeans form ( $dN/dE \propto E^2$ ). This is shown as a dashed line in Fig. 8a. The data, however, are not sufficiently accurate to provide a real verification of this dependence. One difficulty with the self-absorption hypothesis is that it requires rather large distances to the GRB sources<sup>5,6</sup> ( $D > 20$  kpc) and consequently also large burst energies ( $> 10^{40}$  ergs) for those GRB's in which turnovers are observed. Liang *et al.*<sup>6</sup> have interpreted the data in Fig. 8b as evidence for first and second harmonic emission. If the temperature is low enough, one expects to see such emission features. Caution should, however, be exercised with such interpretations since the channel resolution of the data in the critical region ( $E < 100$  keV) is quite crude.

The preceding discussion has shown that all three models are capable of adequately fitting most of the data. This point is further illustrated in Fig. 9 which is reproduced from Liang<sup>6</sup>. Here all three model spectra have been fit to a single event. Below 1 MeV the models are virtually indistinguishable. Above 1 MeV the TS model seems to produce a somewhat harder spectrum than the other two.

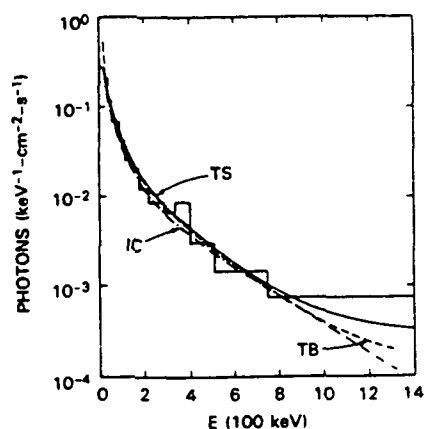


Fig. 9. Comparison of TB, TS and IC fits to the spectrum of GB780918 (from Ref. 6). Original data is from KONUS.

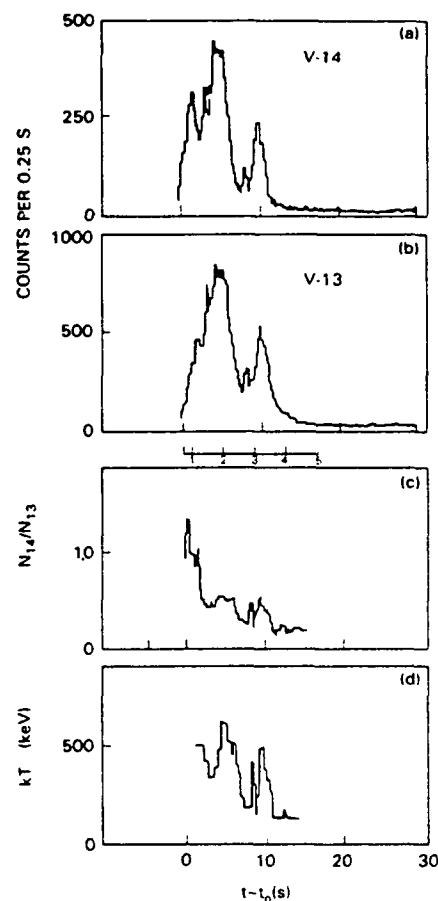
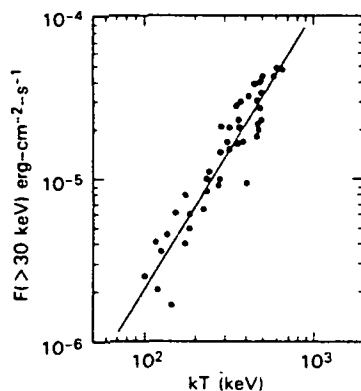


Fig 10. KONUS time-history data from the event GB820827c (from Ref. 8). a) Venera 14 count rate. b) Venera 13 count rate. c) Ratio of Venera 14 to Venera 13 rates. d) Radiation temperature derived from Venera 13 and 14 rates assuming simplified TB spectral form.

The existence of rapid variability in the shape of GRB continuum spectra has recently become evident. Fig. 10 illustrates this behavior for GB820827c<sup>8</sup>. Figs. 10a & b give count rates from the KONUS experiments on Venera 13 & 14, respectively. Because of a gain shift the energy window of the Venera 14 instrument (150-700 keV) is higher than that of the Venera 13 instrument (30-180 keV).

This is a fortunate accident in that it allows one to derive a hardness ratio as a function of time with the relatively high time resolution (0.25 sec) of these two count rates. (The time resolution of the accumulated spectra is 4 sec.) Fig. 10 shows that strong variability in this ratio exists on time scales at least as short as the 0.25 sec., the instrumental limit. From these data Mazets and co-workers have derived the temperature as a function of time assuming the simplified TB spectral form ( $dN/dE \propto (1/E)\exp(-E/kT)$ ). This temperature is plotted as a function of time in Fig. 10d. Fairly rapid and dramatic variations in the temperature are evident.



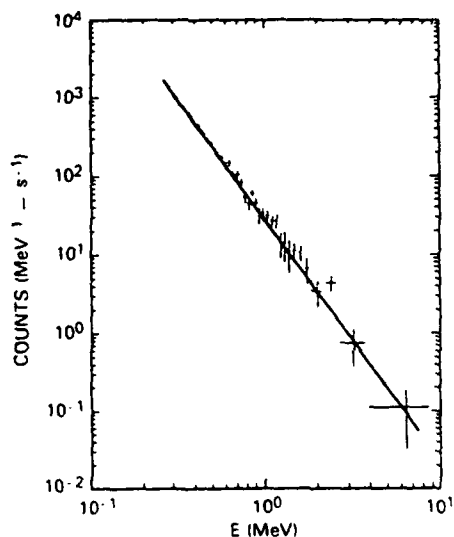
In Fig. 11 the energy flux is derived from the Venera 13 & 14 count rates of Figs. 10a & b and plotted as a function of  $kT$ . The data show a remarkably strong correlation between luminosity and temperature. The form of the dependence derived from this plot is  $L \propto F \propto kT^{1.65 \pm 0.10}$ . That such a strong correlation should exist is quite surprising since the luminosity depends not only on the temperature, but on the volume and density of the emitting region as well. In the TB model (see equation 1) we expect that  $L \propto T^{0.5}$ , which apparently conflicts with this result.

Fig. 11. Flux  $>30$  keV plotted as a function of radiation temperature for GB820827c (from Ref. 8). Data are derived from Fig. 10.

Mazets and co-workers<sup>8</sup> have also applied the TS model to this set of data. We recall from the earlier discussion (see equation 4) that the quantity  $E_c \propto BT^2$  determines the shape of the continuum spectrum. A similar correlation is found, as expected, between  $E_c$  and the luminosity,  $L \propto E_c^{1.5 \pm 0.2} \propto (BT^2)^{1.5 \pm 0.2}$ . The theoretical expression for the synchrotron luminosity was given in equation 5. Unfortunately, only two regimes  $kT_e \ll m_e c^2$  and  $kT_e > m_e c^2$  were discussed. It is interesting, however, to examine the magnetic field and temperature dependence for the high temperature limit. It is of the form  $B^2/K_2(1/T)$  ( $K_2 =$  Bessel function,  $T = kT_e/m_e c^2$ ). In the vicinity of  $T = 1$ ,  $K_2(1/T)$  is a slowly varying function of  $T$ . Thus near  $T = 1$  we expect the luminosity to vary roughly as  $B^2 T^2$ . This does not agree with the dependence derived from Fig. 11 ( $L \propto B^{1.5} T^3$ ) but is certainly a better approximation than the TB model. It may be that coupled density and/or volume variations are responsible for this difference.

Significant departures from exponential-like spectra at higher energies ( $>1$  MeV) have been reported by Share et al.<sup>17</sup> Figs. 12a & b give two examples of spectra that are well fit by power laws up to at least 10 MeV. The existence of such high energy gamma-rays has

important implications with regard to the origin of these events.



Above 1 MeV pair-production by photon-photon interactions is expected to become important. If GRB's are still optically thin at these high energies, then it is probably necessary to place them nearby or to produce the high energy photons in a different region than the low energy photons. One possible way around this difficulty is the possibility of beaming at high energies. Because of the directionality of the photon-photon interaction, photons can preferentially escape normal to the surface of the emission region. It may be possible that we are in the

Fig. 12. SMM spectrum of GB811241 (from Ref. 1). This is an example of a power-law GRB spectrum.

direction of the beam for those GRB's in which hard high-energy tails are observed.

#### SPECTRAL FEATURES

##### a) "Cyclotron" Absorption Lines

As discussed earlier, low-energy (30-80 keV) absorption features appear now to be well-established and present in  $\sim 1/3$  of all detected GRB's. In fact, this proportion may turn out to be even larger when more sensitive instruments provide detailed spectral information on a greater fraction of the detected GRB's. By far the most comprehensive body of data on these features comes from the KONUS experiments on Venera 11-14. An example of the evolution of such a "cyclotron" absorption line is given in Fig. 13<sup>8</sup>. Five spectra are plotted for different time intervals during the event. The absorption feature is quite pronounced during the first second of the event (spectrum A) and subsequently broadens and weakens during the later stages of the event. This type of behavior is quite common in GRB's.

Fig. 14 is another example of structure in the low-energy portion of a GRB spectrum. Mazets et al.<sup>8</sup> have interpreted these data as evidence for a second harmonic seen in absorption. It appears as if it could also be explained as an emission feature superimposed on a continuum spectrum that is somewhat flatter than the TB form that was assumed.

There appear to be some difficulties with the "cyclotron" line interpretation discussed above. If we consider, first, the IC model, magnetic fields of  $B < 10^9$  gauss are required or synchrotron emission will dominate<sup>3</sup>. This conflicts directly with the

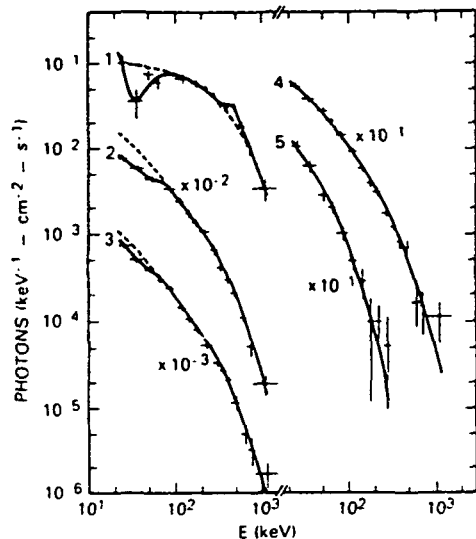


Fig. 13. KONUS spectra from the event GB820827c (from Ref. 8). Spectrum 1 is the first one-second interval of the event. Spectra 2-5 are subsequent for 4 sec. intervals. The radiation temperatures for each of these are: 1, 325 keV; 2, 400 keV; 3, 340 keV; 4, 300 keV; 5, 65 keV.

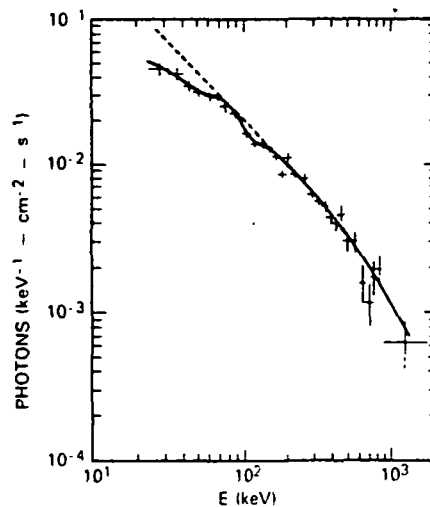


Fig. 14. KONUS spectrum of the event GB820406a (from Ref. 8). Solid line is  $dN/dE \propto E^{-1} \exp(-E/1620)$ .

hypothesis that these features are due to cyclotron absorption. For the TS model, if all the emission comes from a single region with a unique value of  $B$  then no radiation is expected below the first harmonic. However, many of the events displaying absorption features also show emission well below the feature. This would appear to require that the continuum be produced in a region of lower  $B$  than that where the absorption takes place. Such a scenario seems unlikely. Lamb<sup>16</sup> and Norris<sup>18</sup> have suggested a time varying low-energy cut-off as a possible alternate explanation for the "cyclotron" features. It does appear, however, that a rather special set of conditions are required. Whether such conditions are common enough to cause absorption features in  $\sim 1/3$  of all GRB's is not at present clear. Obviously, improved instruments with better time resolution for spectral analysis are needed to answer this question.

#### b) "Annihilation" Lines

Emission features in the 400-500 keV range have been seen in  $\sim 5\%$  of GRB's. These have been interpreted as red-shifted annihilation radiation produced near the surface of a neutron star. For reviews of these features the reader is referred to

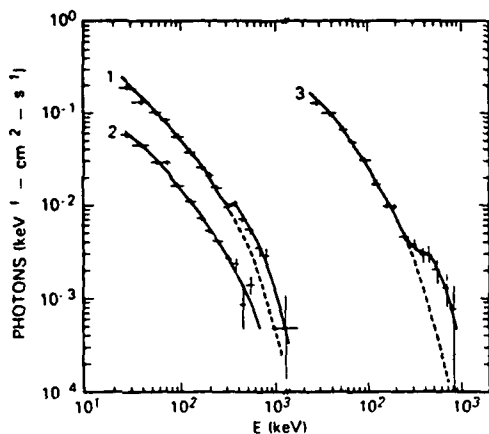


Fig. 15. KONUS spectra from the event GB811231a (from Ref. 8). The second and third spectra show emission features at  $E \sim 400$  keV with high-energy tails.

in a sample of 60 GRB's. No such lines were found at a significance  $>2\sigma$ .

Finally, there is a new result from the KONUS experiment. Fig. 15 shows three spectra from GB811231a for different time intervals throughout the event<sup>8</sup>. The second and third of these spectra display broad emission features at  $\sim 400$  keV each with a pronounced tail extending towards higher energies. It is interesting that this feature appears later in the event rather than at the onset, which is the usual case.

#### CONCLUSION

The general question of the validity of GRB spectral features has been examined and the following conclusions reached: 1) Broad low-energy absorption features may disappear if a flatter continuum spectrum is assumed. 2) Narrow low-energy absorption features appear to be real and have been confirmed in at least two other experiments. 3) "Annihilation" lines are difficult to explain away as spectral artifacts, but a solid confirmation does not yet exist.

A variety of models appear capable of reproducing the behavior of GRB continuum spectra. These include thermal brehmsstrahlung (TB), inverse Compton (IC), and thermal synchrotron (TS). Observations have shown that GRB spectra undergo rapidly variability in hardness. Present instrumentation is, in general, inadequate to accurately track these variations. It has been shown that, in at least a few events, there is a strong correlation between the spectral hardness and the flux or luminosity. Hard power-law tails have been observed in the spectra of a number of GRB's<sup>17</sup>. The power-law behavior continues in some cases to at least  $E = 10$  MeV. To produce an apparently optically thin spectrum at such high

papers by Mazets et al.<sup>7,8</sup> and Teegarden<sup>10</sup>. The principal source of data on these features has again been the KONUS experiments on Venera 11-14. Examples of two of the KONUS spectra were given in Fig. 4. As discussed earlier, no firm confirmation of these results is presently available. The SMM gamma-ray experiment has, however, produced some interesting results relating to the "annihilation" lines. Nolan et al.<sup>1</sup> have reported a weak ( $2.5\sigma$ ) feature at 475 keV in the event GB811231. In addition they have performed a search for narrow ( $<75$  keV) lines in the 350-550 keV range

energies is a difficult problem.

Features in GRB spectra continue to be observed. Low-energy absorption lines ( $30 < E < 80$  keV) have been interpreted as due to cyclotron absorption. Understanding this in the context of the various continuum models appears, however, to be difficult. An alternative suggestion that these features may be due to a time-varying low-energy cut-off has been put forward by Lamb<sup>16</sup> and Norris<sup>18</sup>. Further observations of broad features at higher energies (400-500 keV) have been reported by Mazets and co-workers<sup>8</sup>. A search for narrower lines ( $< 75$  keV) in this same energy range using SMM data has yielded a null result<sup>1</sup>.

#### REFERENCES

1. P. L. Nolan, G. H. Share, D. J. Forrest, E. L. Chupp, S. Matz and E. Rieger, "Positron-Electron Pairs in Astrophysics", ed. M. L. Burns, A. K. Harding and R. Ramaty (AIP, New York, 1983), p. 59.
2. E. P. Mazets, V. V. Golenetskii, V. N. Illinskii, Yu. A. Guryan, R. L. Aptekar, V. N. Panov, I. A. Sokolov, Z. Ya. Sokolova and T. V. Kharitonova, *Astrophys. Space Sci.*, 82, 261 (1982).
3. E. E. Fenimore, R. W. Klebesadel, J. G. Laros, R. E. Stockdale and S. R. Kane, *Nature*, 297, 665 (1982).
4. E. P. Liang, *Nature*, 299, 321 (1982).
5. E. P. Liang, *Ap. J.*, 268, L89 (1983).
6. E. P. Liang, T. Jernigan and R. Rodrigues, *Ap. J.*, 271, 766 (1983).
7. E. P. Mazets, S. V. Golenetskii, R. L. Aptekar, Yu. A. Guryan and Y. N. Il'inskii, *Nature*, 290, 378 (1981).
8. E. P. Mazets, S. V. Golenetskii, Yu. A. Guryan, R. L. Aptekar, V. N. Il'inskii and V. N. Panov, "Positron-Electron Pairs in Astrophysics", ed. M. L. Burns, A. K. Harding and R. Ramaty (AIP, New York, 1983), p. 36.
9. B. J. Teegarden, and T. L. Cline, *Ap. J.* 236, L67 (1980).
10. B. J. Teegarden, "Gamma-Ray Transients and Related Astrophysical Phenomena", ed. R. E. Lingefelter (AIP, New York, 1982), p.123.
11. E. E. Fenimore, R. W. Klebesadel and J. G. Laros, *Proceedings of XXIV COSPAR Meeting (Ottawa, Canada, May 1982)*.
12. B. R. Dennis, K. J. Frost, A. L. Kiplinger, L. E. Orwig, U. Desai and T. L. Cline, "Gamma-Ray Transients and Related Astrophysical Phenomena", ed. R. E. Lingefelter (AIP, New York, 1982), p. 153.
13. G. J. Hueter and D. E. Gruber, "Accreting Neutron Stars", ed. W. Brinkermann and J. Trumper (MPE Report 177, Garching, W. Germany, 1982), p. 213.
14. D. A. Gilman, E. Metzger, R. H. Parker, L. Evans and J. I. Trombka, *Ap. J.*, 236, 951 (1980).
15. J. L. Matteson, Ph.D. Thesis, Univ. of California at San Diego (1972).

16. D. Q. Lamb, "Gamma-Ray Transients and Related Astrophysical Phenomena", ed. R. E. Lingenfelter (AIP, New York, 1982), p. 249.
17. G. H. Share, M.S. Strickman, R. L. Kinzer, E. L. Chupp, D. J. Forrest, J. M. Ryan, E. Rieger, C. Reppin, G. Kanbach, Proceedings of the 17th International Cosmic Ray Conference, Paris, 1981.
18. J. P. Norris, Ph.D. Thesis, Univ. of Maryland, 1983.
19. C. Barat, "Positron-Electron Pairs in Astrophysics", ed. M. L. Burns, A. K. Harding and R. Ramaty (AIP, New York, 1982) p. 54.
20. R. Ramaty, R. E. Lingenfelter and R. W. Bussard, *Astrophys. Space Sci.*, 75, 193 (1981).

## FREQUENCY OF FAST, NARROW GAMMA-RAY BURSTS AND BURST CLASSIFICATION

J. P. Norris\*, T. L. Cline, U. D. Desai, and B. J. Teegarden  
NASA/Goddard Space Flight Center, Greenbelt, Maryland 20771

### ABSTRACT

Evidence from the Vela satellites<sup>1</sup> that very brief,  $\sim 0.1$  s, gamma-ray bursts constitute a class distinct from the longer, highly structured bursts has been strengthened by the results of the Venera 11 and 12 KONUS experiments<sup>2</sup>. The Goddard ISEE-3 Gamma-Ray Burst Spectrometer, utilizing a trigger criterion which is more likely to be independent of duration than previous experiments, has detected a sample of events which enhances this bimodal distribution. The ISEE-3 result is corroborated by an increase in the frequency of detection of short bursts in the KONUS 13/14 database over KONUS 11/12, an effect attributable to the use of a shorter trigger integration time in the later experiments. Considerations such as repeating bursters complicate a simple dichotomous classification of gamma-ray bursts.

### INTRODUCTION

Early studies of the time-histories of the gamma-ray burst events reported by the Vela satellites led to the speculation that very brief,  $\sim 0.1$  s, bursts formed a class distinct from the longer, highly structured bursts<sup>1</sup>. Results of the "KONUS" experiments on Veneras 11, 12, 13, and 14 argue for the existence of a separate class of short duration gamma-ray bursts, revealing that many of the short bursts exhibit much softer spectra ( $\sim 30$  keV) than the more familiar complex bursts. Burst source positions determined with the KONUS experiments indicate that some of these events originate from repeating sources: the localizations for 12 events are consistent with the small error box<sup>3</sup> determined for the famous 5 March 1979 event (source = B0520 -66), and 3 events were apparently produced by another source, designated B1900 +14<sup>2</sup>. The burst recurrence intervals for these two sources range from  $\sim 1$  day to 1 or 2 months.

Several aspects of the observations complicate this seemingly coherent picture of a class of repeating sources which produce short bursts with soft spectra. First, other sources of short bursts with determined positions apparently do not repeat on time scales  $\lesssim 1$  year<sup>2,4</sup>. Second, whereas the characteristic full-width half-maxima (FWHM) of these "single-spike" bursts is  $\sim 0.01$  to  $0.2$  s, the time profiles of some bursts from B0520 -66 were "flat-topped" with durations as long as  $1.5$  s and  $3.5$  s<sup>3</sup>. Third, some bursts, for example 2 November 1978 and 13 June 1979<sup>5,6</sup>, commence with an initial narrow spike but continue for up to several seconds with a low amplitude profile. The time profiles suggest the "tip of the

\* also Department of Physics and Astronomy, University of Maryland, College Park, Maryland 20742; present address: Code 4121.3, Naval Research Laboratory, Washington, DC 20375.

iceberg" effect: these bursts may be of the longer duration, complex variety and only marginally detected. Fourth, in the case of the 6 April 1979 burst, a single-spike event with FWHM  $\sim 0.16$  s, the spectrum was unusually hard<sup>4,7</sup> compared to most complex burst spectra<sup>8</sup>. Finally, a report of correlations of Venera 11 and 12 spacecraft positions with burst localizations, spectral hardness, and fluence<sup>9</sup>, somewhat compromises the KONUS spectral results. For example, the unfolded spectra derived from the KONUS and SIGNE experiments for the 13 June 1979 event exhibit exponential spectra with characteristic energies of  $\sim 70$  keV and  $\sim 660$  keV, respectively<sup>10</sup>. Although the correlation between short durations and soft spectra is not clear and the observations are in some cases contradictory, the existence of two gamma-ray burst populations is suggested by Figure 1, showing a duration histogram for 24 events detected by our ISEE-3 experiment. The Figure also shows the distribution of 123 KONUS 13/14 events of which 60 were detected by both spacecraft.

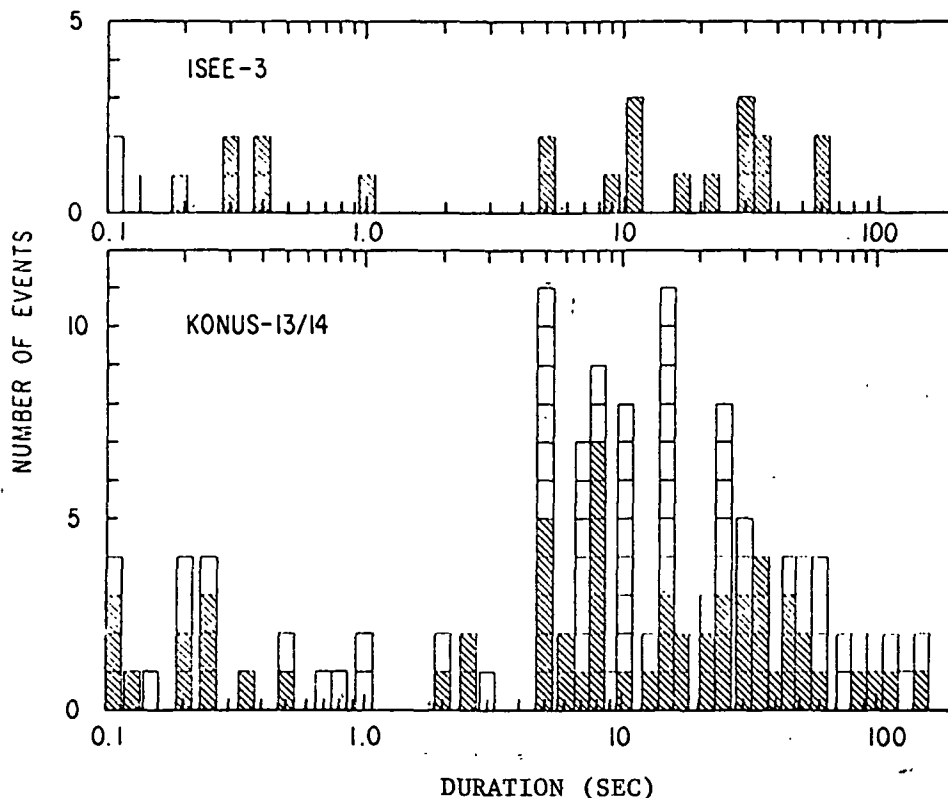


Fig. 1 Distribution of gamma-ray burst durations for ISEE-3 and KONUS-13/14. The shaded areas represent confirmed events, unshaded areas for unconfirmed (one spacecraft only) events. Repeated bursts from the 5 March 1979 source (B0520-66) are not included in the KONUS distribution.

Early experiments, including the Vela network and Helios-2, designed in the late 1960s to mid 1970s, detected only a small number of confirmed short bursts. Thus, their percentage relative to the total number of bursts was ill-defined. In this article we discuss the experiment-specific sampling techniques and point out that the results of the Goddard ISEE-3 Gamma-Ray Burst Spectrometer actually enhance the bimodal distribution suggested in the Vela and KONUS event samples. The implications for burst classification are discussed.

#### ISEE-3 AND KONUS TRIGGER CHARACTERISTICS AND FREQUENCY OF DETECTION OF SHORT BURSTS

The Goddard ISEE-3 Gamma-Ray Burst Spectrometer is described in references 11 and 12. Mainly, two operational detectors in the experiment were responsible for recording gamma-ray bursts. The sensitive element of the principle detector is a high purity germanium crystal with dimensions 4 cm diameter  $\times$  3 cm depth. The detector field-of-view is  $\geq 2\pi$  steradians at energies  $\geq 100$  keV and the detector axis is approximately aligned with the south ecliptic pole, the spacecraft spin axis. The second detector, a cesium iodide scintillator crystal, 3.7 cm diameter  $\times$  2 cm depth, was designed and incorporated into the host cosmic-ray experiment designed by the Max Planck Institute.

The ISEE-3 experiment burst trigger criterion and its philosophy of rate recording both differ from previous techniques in that the time for detecting a preset number of photons is accumulated ("time to spill"), rather than accumulating counts over a preset time interval. The photon count setting (N) and timing precision (pulse frequency) are adjustable by factors of two, within limits. The most often used values have been 32 counts and 1024 Hz. The "time-to-spill" method has the advantage of recording the more intense portions of the temporal history with greater precision. Also, more efficient use of the experiment memory results since fewer memory intervals are wasted on background. In principle, with this method the arrival time of each photon may be recorded with sub-millisecond precision.

The trigger technique also provides a basic new advantage. The conventional detection problem of discriminating against bursts with durations less than the trigger integration time is avoided. Consequently, although the ISEE-3 experiment is not one of the most sensitive contemporary gamma-ray burst sensors, the ISEE-3 event sample may be more representative in that it contains a truer proportion of brief events.

Nine out of twenty-four cosmic events detected by the ISEE-3 experiment from September 1978 to May 1982 exhibited durations less than one second, rise times of tens of milliseconds, and usually no discernable substructure other than an exponential decay in some cases. The 5 March 1979 event<sup>13</sup>, which exhibited an intense initial pulse of FWHM  $\sim 120$  ms (rise time  $< 200$   $\mu$ s), is included in this group since the unique eight-second oscillating decay phase would not have been discernable had the intensity of the initial pulse

been comparable to flux levels ordinarily observed in gamma-ray bursts. The temporal characteristics of the ISEE-3 short events are summarized in Table I. Since the count rate data are generated

Table I ISEE-3 Short Events

Event Dy/Mon/Yr	U.T.C. Hr:Mn:Sc	Peak (cts/s)	Rise Time (s)	FWHM (s)	FWZA
05/MAR/79	15:52:05	32500	< 0.0002	0.12	0.30
15/MAR/79	18:52:15	520	0.03	0.06	0.06
12/MAY/79	21:28:25	420	0.04	0.08	0.08
22/MAR/80	07:21:59	360	0.05	0.36	1.0
06/AUG/80	22:03:31	431	0.06	0.17	0.44
05/DEC/80	09:41:36	607	0.04	0.05	0.19
31/DEC/81	07:58:28	262	0.02	0.30	0.30
08/MAY/82	21:49:55	278	0.06	0.10	0.10
19/MAY/82	11:01:10	910	0.01	0.07	0.40

FWHM, full-width at half-maximum

FWZA, full-width at zero amplitude

using the time-to-spill technique, for a given detector area, the observed rise times and widths are a function of the photon counter setting and clock frequency, the burst intensity, and the intrinsic temporal characteristics. Therefore, for low intensity bursts, the temporal resolution is poor and the observed rise times and widths are probably somewhat longer than the intrinsic times.

Six out of nine of the short ISEE-3 bursts have been confirmed to be of cosmic origin by other spacecraft. For three reasons the remaining events are believed to be genuine gamma-ray burst detections. First, for two of the unconfirmed events, one would need statistical fluctuations, in order to exceed the burst peaks, that would be expected once in  $\geq 27$  years, much longer than the experiment lifetime. Second, in all three unconfirmed events, the duration was  $\leq 0.1$  s. This could possibly explain why the bursts remained undetected by other experiments. Third, the germanium detector, which detected all of the short bursts, is not sensitive to charged particles which simulate spike-like events in cesium iodide scintillators.

The ISEE-3 result has been recently corroborated by an increase in the frequency of detection of short bursts in the KONUS 13/14 database over KONUS 11/12. The KONUS experiments flown on the earlier Venera 11 and 12 spacecraft (see ref. 14) utilized trigger mechanisms with two integration time constants of 0.3 s and 1.5 s, the shorter included to facilitate the detection of fast events. A  $\approx 6\sigma$  rise in either of these rates above a floating background reference rate, sampled at 30 s intervals, signalled the probable onset of a burst and initiated the recording apparatus. As reported by Mazets (pri. comm.), the detector sensitivity is strongly dependent on the event duration. The threshold for detection of events with a given flux increases with decreasing burst duration:

the KONUS detection threshold for bursts of duration less than the trigger integration time is approximately inversely proportional to the duration. The instrumental configurations for the Venera 13 and 14 experiments were similar to the previous KONUS systems<sup>15</sup>. However, the short integration time constant was set at 0.25 s rather than 0.3 s. Upon inspection of the Venera 11/12 and 13/14 data bases, we find that the change in trigger time constants is apparently reflected in a change in the frequency of detection of short bursts. For KONUS 11/12, the ratio of short bursts to total bursts is  $0.07 \pm 0.02$ , whereas for KONUS 13/14, a much higher percentage is indicated,  $0.16 \pm 0.04$ . These figures do not include repeated bursts from the sources B1900 +14 and B0520 -66<sup>2,3</sup>.

#### DISCUSSION

Further corroboration of a significantly higher frequency of short bursts has come from the SIGNE experiments on Venera 11 and 12. Diyachkov et al.<sup>16</sup> report that a distinct class of bursts with durations less than 0.25 s composes 25% of the total, 49 confirmed events. The SIGNE experiments utilized the same trigger integration time as the KONUS 13 and 14 instruments, 0.25 s<sup>17</sup>. If experiments were to employ integration times as short as the average FWHM of short bursts,  $\sim 0.1$  s, the percentage of short bursts then detected may be even higher.

The appearance of a bimodal distribution in Figure 1 suggests that distinct physical processes or different source populations are responsible for the long and short bursts. Since the intensities of short bursts are usually much greater than that of any individual fast fluctuation in the longer, complex bursts, the single-spike short bursts probably do not represent the tip of the iceberg effect. Several considerations complicate this simple dichotomous classification of gamma-ray bursts. Hayles et al.<sup>18</sup> distinguish very short events,  $\sim 0.1$  s, and short events,  $\sim 1$  s, by their characteristic e-folding rise and decay times (rise  $\sim$  decay in both cases),  $\sim 40$  ms and  $\sim 500$  ms, respectively. However, in their Figure 3, a scatter diagram of decay times versus rise times, the data do not appear to clump into two clearly separated domains. Furthermore, since two bursters are known to have produced more than one burst, a range in event durations might be expected from any given source, as has been observed from B0520 -66. On the other hand, whereas the 5 March 1979 event has been suggested as a prototype for the short bursts<sup>2</sup>, the unique characteristics of the 5 March event<sup>13</sup> and the repetitive nature of B1900 +14 and B0520 -66 suggest that the two repeating bursters may represent another distinct class of sources. All eleven bursts from B0520 -66 following the 5 March event and all three bursts from B1900 +14 manifested exponential spectra with characteristic energies  $\sim 35$  keV, much softer than the spectra of the longer, complex events<sup>8</sup>. However, the spectral pattern of the short bursts which are not at present<sup>4,7,9,10</sup> identified with repeating sources appears to be diverse.

These considerations are additional reasons, beyond the well-known instrumental problems, for approaching the construction and interpretation of the Log N(>S) - Log S relationship(s) for gamma-ray burst sources with caution.

We express our thanks to Dr. E. P. Mazets for graciously providing us with unpublished results from the Venera 13 and 14 KONUS experiments.

#### REFERENCES

1. Cline, T. L. and Desai, U. D., "Progress in Gamma-Ray Burst Astronomy" in Proceedings of the 9<sup>th</sup> ESLAB Symposium (ESRO, Noordwijk, 1974), p. 37.
2. Mazets, E. P., Golenetskii, S. V., Guryan, Yu. A. and Ilyinskii, V. N., "The 5 March 1979 Event and the Distinct Class of Short Gamma Bursts: Are They of the Same Origin", Report No. 738 (A. F. Ioffe Physico-Technical Institute, 1981).
3. Cline, T. L., "Gamma-Ray Bursts: A 1983 Overview", these proceedings.
4. Mazets, E. P. and Golenetskii, S. V., "Recent Results of the Gamma-Ray Burst Studies in the KONUS Experiment", Report No. 632 (A. F. Ioffe Physico-Technical Institute, 1979).
5. Mazets, E. P. et al., Astrophys. Space Sci., 80, 3 (1980).
6. Mazets, E. P. et al., Astrophys. Space Sci., 80, 85 (1980).
7. Laros, J. G. et al., Astrophys. J. Lett., 245, L63 (1981).
8. Cline, T. L. and Desai, U. D., Astrophys. J. Lett., 196, L43 (1975).
9. Laros, J. G., Evans, W. D., Fenimore, E. E. and Klebesadel, R. W., Astrophys. Space Sci., 88, 243 (1982).
10. Barat, C. et al. Astrophys. J. Lett. (submitted).
11. Teegarden, B. J. and Cline, T. L., Astrophys. J. Lett., 236, L67 (1980).
12. Teegarden, B. J. et al., in Gamma-Ray Spectroscopy in Astrophysics, (eds Cline, T. L. & Ramaty, R.) NASA TM79619, (1978), p. 516.
13. Cline, T. L., Ann. N. Y. Acad. Sci., 375, 314 (1981).
14. Mazets, E. P. et al., Soviet Astr. Letters, 5, 87 (1979).
15. Mazets, E. P. et al., in Positron-Electron Pairs in Astrophysics, (eds Burns, M. L., Harding, A. K. & Ramaty, R.) AIP Conf. Proc. No. 101, (AIP, New York, 1983), p. 36.
16. Diyachkov, A. V. et al., preprint, (1982).
17. Barat, C. et al., Space Sci. Inst., 5, 229 (1981).
18. Hayles, R. I. et al., "New Results on the Time Histories of Gamma-Ray Bursts" COSPAR/IAU Symposium on Advances in High Energy Astrophysics and Cosmology, Rojen, Bulgaria (1983).

## EQUILIBRIA IN STRONGLY MAGNETIZED PAIR PLASMAS

Alice K. Harding  
NASA/Goddard Space Flight Center, Greenbelt MD 20771

### ABSTRACT

Positron-electron pair densities for a thermal plasma in the steady-state equilibrium where pair production balances pair annihilation are found as a function of temperature  $kT / mc^2 \lesssim 1$ , source size  $R$  and magnetic field strength  $B$ . When the plasma is strongly magnetized,  $B > 10^{12}$  G, the important processes are synchrotron radiation, one-photon (magnetic) pair production and two-photon pair annihilation. An analytic solution for the equilibrium pair density, found under certain simplifying assumptions, shows that optically thin equilibria exist only for sufficiently small source sizes.

### INTRODUCTION

Pair equilibrium in thermal plasmas has been the subject of increasing interest in connection with astrophysical sources observed to emit high energy photons with energies in excess of  $mc^2$ . The behavior of strongly magnetized pair plasmas may be of relevance to models of gamma-ray bursts, and equilibrium solutions would apply if steady acceleration is occurring throughout the source region via a process whose timescale is comparable to the energy loss timescale. Although there have been studies of the properties of non-magnetized or weakly magnetized pair plasmas<sup>1,2,3</sup>, the properties of pair plasmas in strong magnetic fields are virtually unexplored. In the presence of a superstrong field, a different set of processes determines the pair equilibrium. I will present calculations of the equilibrium pair densities from a simple analytic solution to the pair balance equation in the case where only a few processes determine the state of the plasma.

The plasma is considered to occupy a finite, static source region of size  $R$  and to have a temperature in the mildly relativistic regime,  $kT \lesssim mc^2$ . The presence of a superstrong magnetic field allows a number of simplifying assumptions:

1. The only important source of photons is synchrotron radiation from the pairs. Bremsstrahlung and pair annihilation will be negligible sources of photons.
2. One-photon pair production dominates other pair production processes<sup>4,5</sup>.
3. Pair annihilation occurs only by the two-photon process. One-photon annihilation is negligible unless  $B > 10^{13}$  G (Ref. 6).
4. Since bremsstrahlung and other processes involving protons are unimportant, the proton density is indeterminate, and we can assume  $n_+ = n_-$  (or  $n_+ / N \gg 1$ ), where  $n_+$ ,  $n_-$  and  $N$  are the number densities of  $e^+$ ,  $e^-$ , and protons, respectively.

We also make the following additional assumptions:

5. The pairs have an isotropic Maxwellian distribution at temperature  $kT$ .
6. The source region is optically thin to Compton scattering,  $\tau_T = (n_+ + n_-)\sigma_T R < 1$ , pair production,  $\lambda_{1\gamma} > R$ , and synchrotron absorption for photons with  $h\omega > 2mc^2$ . (This assumption can be justified a posteriori).

### EQUILIBRIUM CALCULATION

The equilibrium state of the plasma is determined by three parameters: temperature  $T_* = kT/mc^2$ , magnetic field strength  $B' = B/B_{cr}$  where  $B_{cr} = 4.414 \times 10^{13}$  G, and source size  $R$ . The photon production rate is the thermal synchrotron spectrum for mildly relativistic electrons derived by Petrosian<sup>7</sup>:

$$j_\nu(\theta) = \frac{\pi e^2}{\sqrt{2} 3c} (n_+ + n_-) v K_2^{-1}\left(\frac{v}{T_*}\right) \exp\left[-(4.5 \frac{v}{v_c \sin\theta})^{1/3}\right] \quad (1)$$

where  $\frac{hv}{mc^2} = B' T_*^2$ ,

and  $\theta$  is the angle between the emitted photon and  $B$ .

The photon distribution will be approximated as

$$n_\gamma(E, \theta) = \frac{j_\nu(\theta)}{hv} t_{esc} \quad (2)$$

where  $t_{esc}$  is the escape time of the photons from the source region and is taken to be,  $t_{esc} = R/c$ , since the plasma is assumed to be optically thin. We look for solutions to the equation,

$$\dot{n}_+ = \dot{n}_- = \dot{n}_+^{prod} - \dot{n}_+^{ann} = 0 \quad (3)$$

where the pair densities are the distribution functions for the pairs integrated over energy. The rate of pair production by the one-photon process is,

$$\dot{n}_+^{prod} = \iint n_\gamma(E, \theta) r_{1\gamma}(B', E, \theta) d\Omega dE \quad (4)$$

where  $r_{1\gamma}$  is the rate of pair production per photon of energy  $E$ <sup>8</sup>,

$$r_{1\gamma}(B', E, \theta) = 0.23 \frac{\alpha c}{\chi} B' \sin\theta \exp\left[-\frac{4}{3} \frac{f(E)}{\chi}\right]$$

with  $\chi \equiv \left(\frac{E}{2mc^2}\right) B' \sin\theta$ , (4a)

$$f(E) = 1 + .42 (E \sin\theta / 2mc^2)^{-2.7}$$

The integrand in Eqn (4) is sharply peaked about  $E_0 = mc^2 (32 T_*/3 B' \sin\theta)^{1/2}$  and  $\dot{n}_+^{prod}$  may therefore be evaluated by the method of steepest descents.<sup>5</sup> The two-photon pair annihilation rate in the non-relativistic limit<sup>9</sup>, ignoring effects of the magnetic field, is

$$\dot{n}_+^{\text{ann}} = \pi r_e^2 c n_+ n_- \quad (5)$$

Because  $\dot{n}_+^{\text{prod}}$  goes as  $n_+$  and  $\dot{n}_+^{\text{ann}}$  goes as  $n_+^2$ , with assumption (4) above, the solution to equation (3) is simple and the equilibrium pair density is found to be,

$$n_+ = 2.8 \times 10^{35} R B' T_*^{1/2} e^{1/T_*} \exp \left[ \frac{4}{3} \left( \frac{6}{B' T_*} \right)^{1/2} - \frac{.09 B'^{0.85}}{T_*} \right] \text{cm}^{-3} \quad (6)$$

valid for  $\left( \frac{8}{3} T_* B' \right)^{1/2} < 1$ .

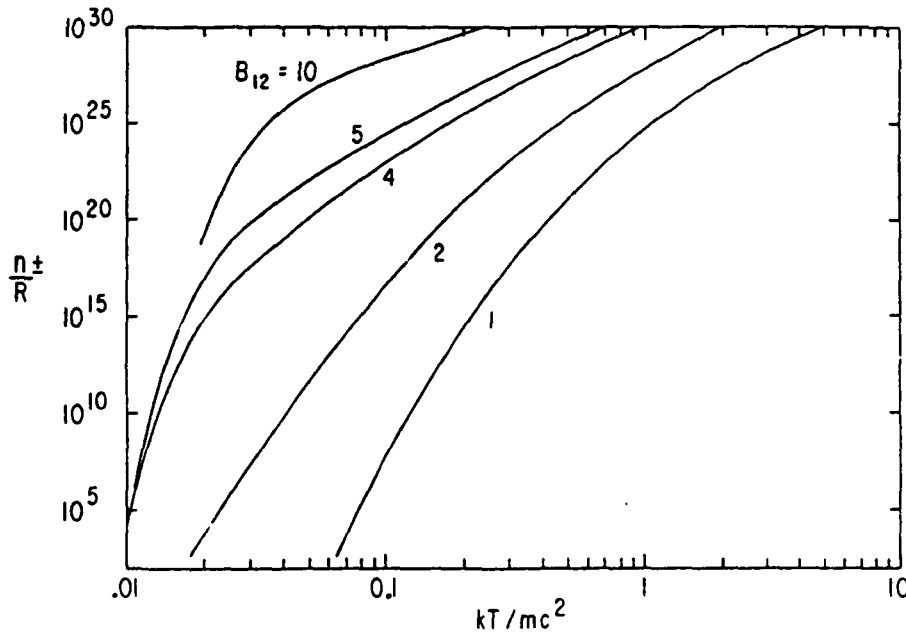


Fig. 1 - Equilibrium pair density divided by source size as a function of temperature and magnetic field strength (in units of  $10^{12}$  G).

The quantity  $n_+/R$  is plotted in Fig. 1 as a function of  $T_*$  and  $B$ . For  $R$  much larger than 1 cm, the pair densities are high enough to violate the assumption that  $\tau_T < 1$ . However, inclusion of Compton scattering will increase the photon escape time, increasing the photon density and pair production rate further. In addition, other photon and pair production processes which have been ignored will also increase the pair density. For the parameter ranges considered here, pairs will be produced faster than they can be destroyed. Unless the plasma is optically thin to Compton scattering, then, it will not remain in a steady state but evolve to a state of thermal equilibrium, where the pair density is equal to the thermal equilibrium pair density at that temperature. Fig. 2 shows the source size required for optically thin equilibrium at a given value of  $T$  and  $B$  (ie. the  $R$  for which  $\tau_T = 1$ ).

For these values of  $R(\tau_T=1)$ , I find that the plasma becomes

optically thick to Compton scattering well before becoming thick to  $\gamma$  pair production, so that assumption (6) is justified. Allowing photons to gain or lose energy through scattering or relaxing the assumption of a Maxwellian distribution for the pairs may change the results, but would require a more detailed numerical treatment and some knowledge of the acceleration mechanism. From these results, one might tentatively conclude that if such strongly magnetized pair plasmas exist in optically-thin equilibrium in gamma-ray burst sources, they must be confined to very small regions or thin layers.

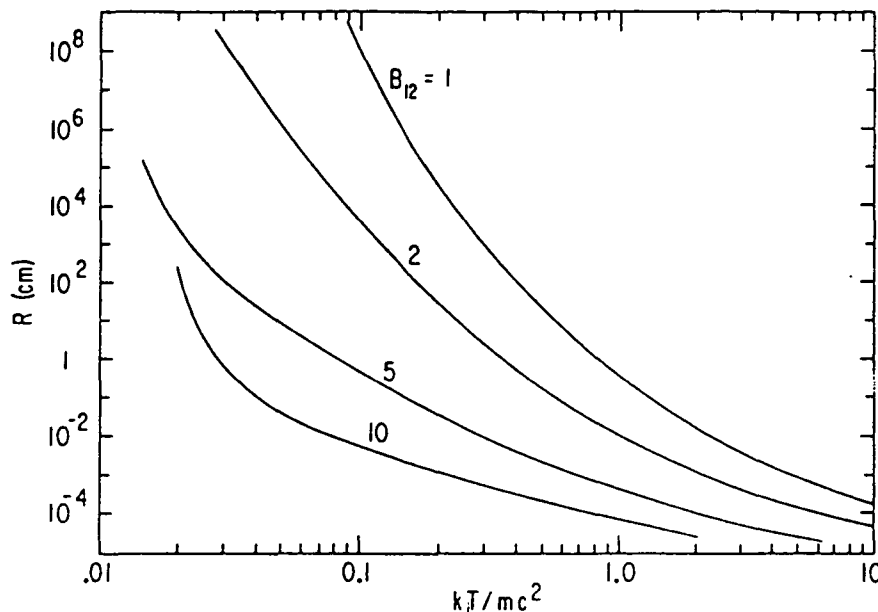


Fig. 2 -  $R(\tau_T = 1)$  as a function of  $kT$  for different magnetic field strengths.

#### REFERENCES

1. A. P. Lightman, *Astrophys. J.* 253, 842 (1982).
2. R. Svensson, *Astrophys. J.* 258, 335 (1982).
3. F. Takahara and M. Kusunose, *Positron-Electron Pairs in Astrophysics*, ed. M.L. Burns, A.K. Harding, R. Ramaty (AIP, New York, 1983), 400.
4. M. L. Burns and A. K. Harding, *Positron-Electron Pairs in Astrophysics*, ed. M.L. Burns, A.K. Harding, R. Ramaty (AIP, New York, 1983), 416.
5. M. L. Burns and A. K. Harding, in preparation.
6. J. K. Daugherty and R. W. Bussard, *Astrophys. J.* 238, 296 (1980).
7. V. Petrosian, *Astrophys. J.* 251, 727 (1981).
8. J. K. Daugherty and A. K. Harding, *Astrophys. J.*, in press (1983).
9. G. S. Bisnovatyí-Kogan, Ya. B. Zeldovich and R. A. Sunyaev, *Sov. Astron.*, 15, 17 (1971).

## IMPLICATIONS OF THE THREE GRB OPTICAL FLASHES

B. E. Schaefer

NASA/Goddard Space Flight Center, Code 661, Greenbelt, MD 20771

Since the discovery of gamma-ray bursters (GRBs) a decade ago, it was realized that the identification of an optical counterpart (either during a burst or during quiescence) would be a significant step forward in our understanding of these enigmatic objects. The reason is that optical data is easier to obtain and can then be related to the large body of already existing optical knowledge. Optical observations promise a large advance in our understanding because we will be looking at GRBs in a way they have never been looked at before. In general, no optical objects have been convincingly associated with any GRB. Two exceptions to this rule have been found, the first of which is the accurate positional coincidence of the 5 March 1979 GRB with a supernova remnant in the Large Magellanic Cloud.

The second exception is a report by Schaefer<sup>1</sup> on the probable identification of a bursting GRB on a 1928 archival photograph from Harvard. The reasons for associating this 1928 image with a GRB are that (1) it appears inside a GRB error region as well as a possibly associated X-ray error region, (2) no object appears at or near the GRB location on photographs exposed immediately before or after the discovery plate, (3) the image is not trailed; whereas all normal star images are trailed by 17", (4) the image shows coma, and (5) the image is not as centrally concentrated as normal star images. Each of these points are exactly what may be expected for a short duration optical flash from a GRB. Despite the strength of this evidence, it is hard to calm all worries that this image could be caused by some extraordinary fluke of nature.

One way to eliminate these fears is to locate more optical transient images. To this end, Barat et al.<sup>2</sup> and Cline et al.<sup>3</sup> have used the international network to determine several new precise GRB positions. These positions were searched for transient images on the Harvard archival plate collection. Two additional optical transient images have been identified in two GRB error regions on plates exposed in 1901 and 1944. A detailed discussion of these results will appear in Schaefer et al.<sup>4</sup>. In the spirit of this conference, this paper will discuss the implications of these observations while avoiding detailed arguments.

The finding of three optical transients argues against the "extraordinary fluke" explanation. In addition, a control experiment was performed, in which no transient images were found on the Harvard plates in a search of areas which contained no known GRBs. This region was 34.3 times larger than the region examined which was known to contain a GRB. If the three transient images found inside the GRB were due to some background source, then roughly a hundred transient images should have been found in the control region. This statistical argument, when combined with the positive evidence from analysis of the plates, satisfactorily demonstrates that the optical transients are both real and associated with GRBs.

Similarly to the case for the 1928 transient, the 1901 optical transient image was circular in shape on an 11-minute exposure which was trailed by 8". From these figures and the image width, the optical duration is deduced to be less than roughly 3 minutes. The shallow slope of the profile of the 1928 transient image indicates that the flash duration is under 10 seconds. In addition, significant limits can be placed on the presence of any optical precursors or afterglows.

The optical fluence ( $E_{opt}$ ) from the three optical transients can be measured from the Harvard plates. Schaefer and Ricker<sup>5</sup> used this measured  $E_{opt}$  (along with conservative temperature and distance limits and the assumption that the optical light is emitted by a thermal mechanism) to show that the size of the optical emitting region is much larger than the size of the gamma-ray emitting region. This implies that some large object, in addition to the neutron star, must be in the GRB system. A possible source of the optical light could be the reprocessing of gamma-rays off a companion star or an accretion disc.

The modern gamma-ray fluence ( $E_{\gamma}$ ) can be combined with the  $E_{opt}$  from archival data to form the ratio  $E_{\gamma}/E_{opt}$ . For the three optical transients, this ratio is measured to be 800, 900, and 900, while  $E_{\gamma}$  varies by a factor of 25. This result suggests that the ratio is a constant, although clearly more observations are needed. If this suggestion is true, then it seems probable that (1)  $E_{\gamma}/E_{opt}$  is constant from GRB to GRB and from burst to burst, and (2)  $E_{\gamma}$  is a constant from burst to burst for a given GRB. The first condition is violated if the radiation pattern of gamma-ray or optical light is non-spherical. An example of this could be that the fraction of optical light which reaches Earth (after reprocessing off a companion star or an accretion disc) will vary with the companion's orbital phase or the disc's inclination. Many proposed GRB models have difficulty fulfilling the second condition.

A total exposure of 2.7 years was examined on the Harvard plates and three optical transients were found which are associated with GRBs. This implies an optical transient recurrence time scale of roughly once per year for each GRB. Presently, it is unclear whether this optical time scale is consistent with the possibly longer gamma-ray recurrence time scale. Even if the gamma-ray time scale is within several orders of magnitude of the optical time scale, this would be a severe blow to many GRB models which either do not allow for recurrence or predict very infrequent outbursts. Should the two time scales prove to be different, this could be explained either by a gamma-ray luminosity function or by the existence of two classes of transients from GRBs.

The accurate positions for the bursting GRB counterparts allow for very deep searches for the quiescent GRB counterparts. Pedersen et al.<sup>6</sup>, and Schaefer, Seitzer, and Bradt<sup>7</sup> have reported several "unusual" objects ( $m \sim 24$ ) inside the 1928 optical error box. The presence of more than one candidate indicates that it may be difficult to identify which one (if any) is the true counterpart. It is hoped that the 1901 and 1944 optical error boxes will be found to contain only one candidate. The optical study of any such candidates may well provide the long awaited description of the

nature of the GRB system. Searches of these boxes are currently underway.

Optical studies of GRBs have provided data on the duration, fluence,  $E_\gamma/E_{\text{opt}}$ , optical recurrence time scale, presence of optical precursors or afterflows, and has allowed several quiescent GRB candidates to be identified. Many problems remain; for example, London and Cominsky<sup>8</sup> have demonstrated that a simple model where the gamma-rays are reprocessed on a companion star will not yield enough optical energy. Detailed modelling of archival gamma-ray data or of new data from Veneras 13 and 14 may accurately determine the gamma-ray recurrence time scale. If  $E_\gamma/E_{\text{opt}}$  for several additional optical transients can be measured, then the constancy of this ratio can be confirmed or denied. Continued monitoring of the optical GRB error boxes is needed to identify quiescent GRB counterparts. It may be expected that within several years these problems will be solved and our understanding of GRBs greatly deepened.

#### REFERENCES

1. B.E. Schaefer, Nature 294, 722 (1981).
2. C. Barat et al., Ap. J. Lett. submitted (1983).
3. T. L. Cline et al., Ap. J. Lett. submitted (1983).
4. B. E. Schaefer et al., Ap. J. Lett. submitted (1983).
5. B. E. Schaefer and G. R. Ricker, Nature, 302, 43 (1983).
6. H. Pedersen et al., Ap. J. Lett. 270, L43 (1983).
7. B. E. Schaefer, P. Seitzer, and H. V. Bradt, Ap. J. Lett. 270, L49 (1983).
8. R. London and L. Cominsky, Ap. J. Lett. submitted (1983).

THE RAPIDLY MOVING TELESCOPE:  
AN INSTRUMENT FOR THE PRECISE STUDY OF OPTICAL TRANSIENTS

B.J. Teegarden, T.T. von Roseninge, T.L. Cline, and R. Kaipa  
Goddard Space Flight Center, Greenbelt, MD

ABSTRACT

We have initiated at the Goddard Space Flight Center the development of a small telescope with a very rapid pointing capability whose purpose is to search for and study fast optical transients that may be associated with gamma-ray bursts and other phenomena. The primary motivation for this search is the discovery by Schaefer<sup>1</sup> of the existence of a transient optical event from the known location of a gamma-ray burst. The telescope will have the capability of rapidly acquiring any target in the night sky within 0.7 second and locating the object's position with  $\pm 1$  arcsec accuracy. The initial detection of the event will be accomplished by the MIT Explosive Transient Camera<sup>2,3</sup> or ETC. This will provide rough pointing coordinates to the RMT on the average within  $\sim 1$  second after the detection of the event.

INTRODUCTION

The occurrence of an optical flash in association with the position of a known gamma-ray burster was discovered through an archival plate search by Schaefer<sup>1</sup>. Since then, Schaefer has found two more candidate events by the same method<sup>4</sup>. These flashes were quite bright ( $m \approx 3-6$  assuming a 1 second duration). All three events were consistent with a gamma-ray to optical luminosity ratio  $L_\gamma / L_{opt} \approx 800$  (with, of course, the caveat that the optical and gamma-ray measurements were not contemporaneous). Subsequent deep searches of these optical transient error boxes have not yet yielded an identification of the quiescent optical counterpart. The first discovered event (corresponding to the 19 Nov. 1978 gamma-ray burst) has been the most extensively studied. The error box for this event has been subjected to deep CCD searches by Pederson et al.<sup>5</sup> and Schaefer et al.<sup>6</sup> Their combined results have yielded four candidate objects, two of which appear to be variable. The magnitudes of these candidate objects are in the  $m = 23-25$  range. (The limiting magnitudes of the exposures were typically  $m = 25$ ). These searches are complicated by the fact that significant proper motion is possible between the time of the optical flash detection and the contemporary gamma-ray measurement. A more precise determination of the position of the flash is desirable and perhaps necessary to obtain an unambiguous identification of the quiescent counterpart. The absence of a quiescent optical counterpart with  $m < 23$  poses a major problem for burst models. The usual scenario for the production of visible radiation (e.g. in X-ray bursters) is through reprocessing the high energy radiation in either an accretion disk or in the atmosphere of a companion star<sup>7</sup>. In X-ray bursters the emission of visible light is typically delayed by  $\sim 2$  seconds from the X-ray emission<sup>7</sup>. The present limit of  $m > 23$  means that for an assumed gamma-ray burster distance of 1 kpc, the absolute magnitude

of the companion would have to be  $M > 13$ . This is a problem for models that are based on binary systems since the companion would then have to have a very low luminosity.

Because of the faintness of the quiescent optical counterpart it is vitally important to localize the burster with great accuracy. Unambiguous identification of objects fainter than  $m = 23$  will generally require positions with arcsec accuracy. (Averaged over the celestial sphere we may expect very roughly  $20 \text{ arcsec}^2/\text{star}$  with  $m < 23$ ). To this end we have designed an instrument with the capability of rapidly acquiring a gamma-burst source and determining its position to at least  $\pm 1 \text{ arcsec}$ . The Rapidly Moving Telescope (RMT) is a companion to the Explosive Transient Camera (ETC) described elsewhere in these proceedings<sup>3</sup>. The basic idea is that the ETC detects an optical transient in real time and transmits its rough coordinates to the RMT. The RMT then rapidly slews to the source and makes precise measurements of the light curve and position. Eventually the system may be upgraded to do spectroscopy as well. The technical features and expected performance of the RMT are described in detail in the following sections.

#### INSTRUMENT DESCRIPTION

The RMT is shown schematically in Fig. 1. It consists of a 17.8 cm diameter telescope looking vertically downward onto a mirror

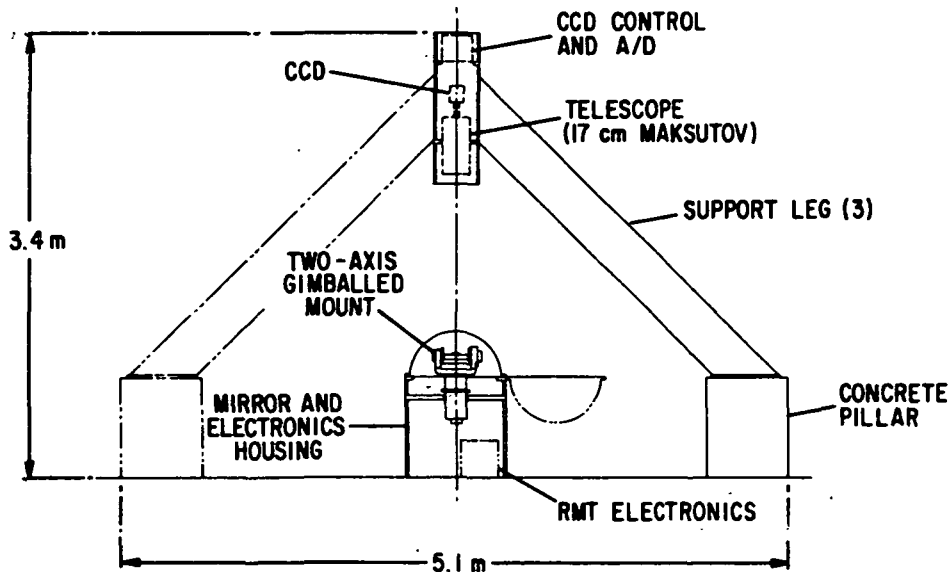


Figure 1. Schematic of telescope, gimbal mount and enclosures.

which is supported by a motorized 2-axis gimbal mount. Rotation of the mirror over a 90 degree range in elevation and a 180 degree range in azimuth allows viewing of all the sky except for 4% that is blocked by the telescope and its support legs. When the ETC detects an optical transient, it sends the corresponding coordinates in R.A. and Dec. to the RMT overseer computer. These coordinates will be accurate to at least a few arcmin, sufficient to bring the source

within the 17 x 12 arcmin RMT field-of-view. The overseer computer then initiates independent slew modes for the elevation and azimuth axes. Following acquisition of the source, the mirror continues to move in a sidereal tracking mode. Images from a CCD camera at the RMT focus are gathered 1 per second and, together with UT and the mirror position angles, are saved on disk. This is continued for ~ 100 seconds, following which the event data is written onto magnetic tape. The primary characteristics of the RMT are summarized in Table 1. and will now be discussed in further detail.

Table 1

## RMT Characteristics

<b>GIMBAL MOUNT</b>		
Maximum velocity:	azimuth-250 deg/sec	elevation-170 deg/sec
Maximum slew time:	azimuth-0.7 seconds	elevation-0.5 seconds
Position accuracy:	±2.5 arcsec (3 sigma)	
Position stability:	<±1 arcsec	
<b>MIRROR</b>		
Dimensions:	18.9 cm x 25.4 cm	
Flatness:	Lambda/4	
<b>TELESCOPE</b>		
Type:	17.8 cm diameter Maksutov-Cassegrain	
Focal length:	2540 mm	
Field of view:	17 arcmin x 12 arcmin	
Optical throughput:	~ 0.8 average from 3500 - 7000 Å	
<b>CCD</b>		
Type:	Texas Instruments 584x390	
Dimensions:	1.29 cm x .86 cm	
Pixel size:	22 microns x 22 microns	
Readout time:	1 sec	
Integration time:	1 sec	
Readout noise:	~20 e rms per pixel	
Operating temperature:	-60 degrees Celsius	
Quantum Efficiency:	0.75 @ 6000 Å	

The two-axis gimballed mount and its mirror are depicted in Fig. 2. Each axis has a brushless drive motor and a differential optical shaft-angle encoder. Two TI9995 microprocessors under control of the overseer computer are used to independently control each axis. The shaft-angle encoders provide a zero reference pulse, sine and cosine outputs (with ~ 1 arcmin period), and motor commutation signals. The cosine signal is provided along with the sine in order to determine the direction of shaft rotation. Zero crossings of these signals produce pulses which are counted in an up/down counter which provides a measure of the shaft position to one part in  $2^{16}$ , i.e. to 20 arcsec. This counter is initialized using the zero reference pulse when the system is first powered up.

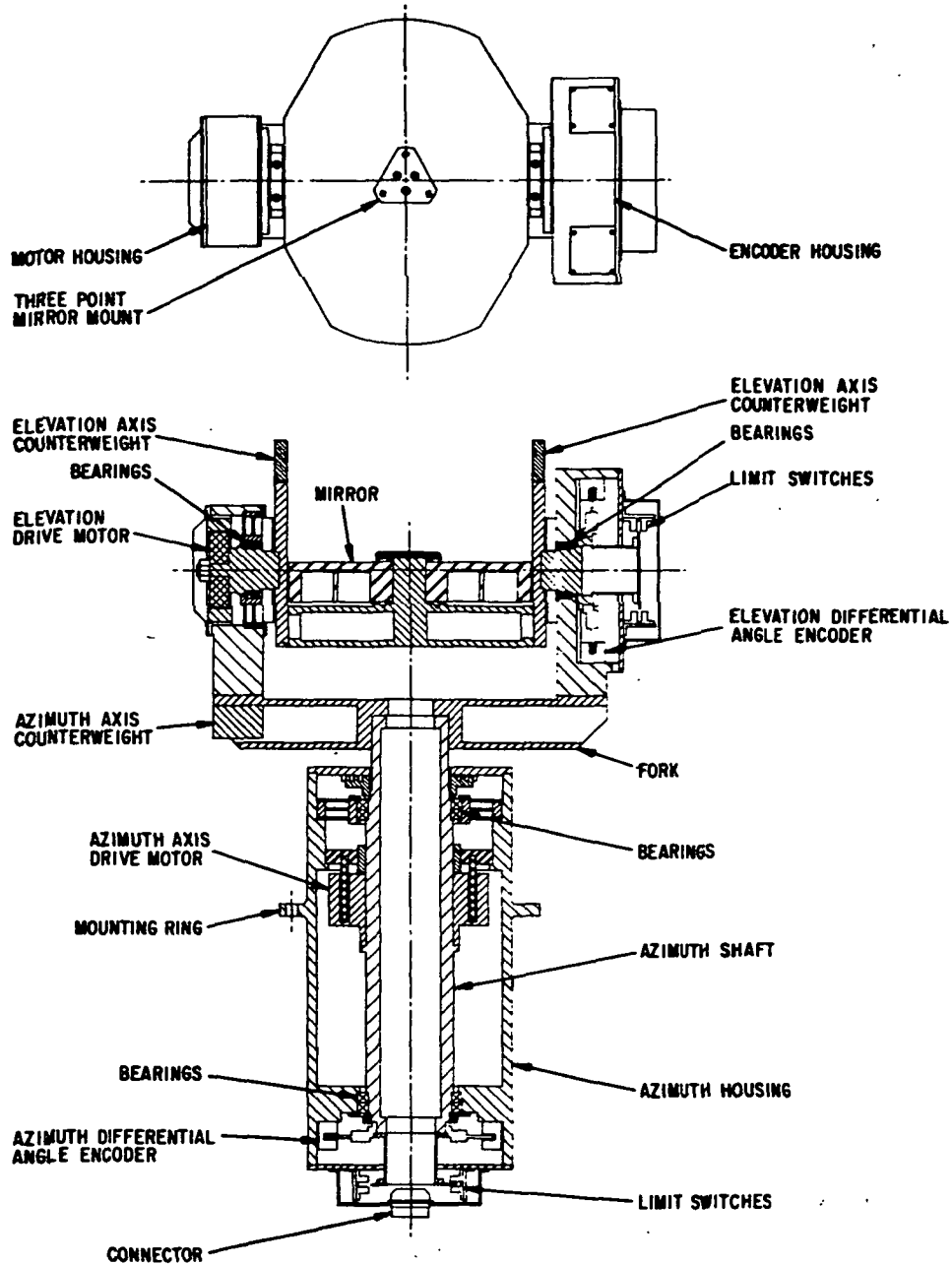


Figure 2. Two-axis gimbal mount..

The sine and cosine signals are then digitized by a fast 8-bit ADC to increase the angular resolution to  $2^{22}$  (0.3 arcsec). The maximum absolute error of the encoders is specified to be  $\pm 2.5$  arcsec (3 sigma) while the error change over any 5 degree segment should not exceed  $\pm 1$  arcsec. The angular velocity must be measured for each axis over an extremely wide range ( $\sim 10^6$ ) since we require both accurate tracking at the sidereal rate (15 arcsec/sec) and rapid

slewing (250 degrees/sec). In the low angular velocity range ( $\leq 5$  arcmin/sec) this is done by a simple analog computer to convert the sine and cosine signals into a voltage proportional to the angular velocity. This voltage is used in the active control loop which determines the motor drive current. In the high angular velocity regime, the position counter is used to determine velocity digitally.

The mirror is light-weighted and quasi-elliptical with a minor axis of 18.9 cm and major axis of 25.4 cm. It is front-surface aluminized and flat to  $1/4$  wavelength. The RMT telescope is a ruggedized Questar model 20019. It has a clear aperture of 17.8 cm and a focal length of 2540 mm. The Texas Instruments 584x390 element CCD has a pixel size of 22 microns. Hence the total field-of-view is  $17 \times 12$  arcmin, and the pixel size is  $1.8 \times 1.8$  arcsec. Eventually a Barlow lens may be used to reduce the pixel angular size. The CCD will be identical to the ones used by the ETC. It will be cooled to  $-60^\circ\text{C}$  to reduce its internal noise.

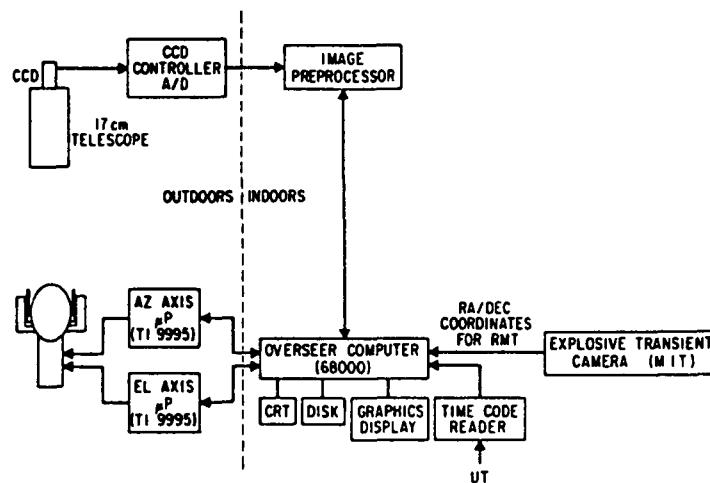
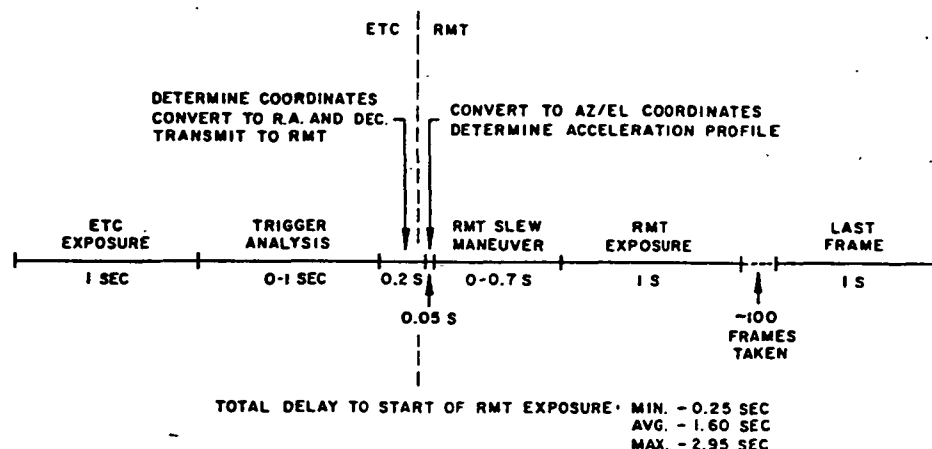


Figure 3. RMT block diagram.

Fig. 3 shows a block diagram of the overall data-gathering and control system. It also shows which portions are located outdoors and indoors. The CCD preprocessor and the overseer computer are essentially the same as those in the ETC. The preprocessor performs the operations of field-flattening and thresholding and transmits the compressed data to the overseer computer. There the data is stored on disk and eventually dumped to magnetic tape. The overseer also converts R.A. and Dec. from the ETC to azimuth and elevation coordinates for source acquisition. It also provides coordinates and times often enough so that the TI9995 slave microprocessors can linearly interpolate and maintain accurate sidereal tracking. It can acquire the data necessary to display time histories of the acceleration, velocity and position of each axis.

## RMT PERFORMANCE

One of the most critical RMT parameters is the maximum source acquisition time. From Table 1, one finds a worst case source acquisition time of 0.7 seconds. This corresponds to a slew of 90 degrees in azimuth and 45 degrees in elevation. A time-line for the combined ETC/RMT detection/acquisition sequence is given in Fig. 4. The ETC CCD accumulates photons during a 1 second exposure and



## ETC/RMT TIME LINE

Figure 4. ETC/RMT time line.

is read out during the following second. The actual time during this trigger analysis period when the optical flash is detected is determined by its position in the read-out sequence and may be anywhere from 0 to 1 second. Subsequent delays occur for coordinate transformations, and initialization of the RMT slew maneuver. Following completion of the slew maneuver, the RMT immediately begins a sequence of CCD exposures of the target area. This sequence is presently planned to be 100 1-second exposures, but can be easily changed. As discussed in the preceding section, the angular position of the 2-axis gimbaled mount is obtained by interpolation of the quasi-sinusoidal outputs of the differential angle encoder: The deviation from a true sine wave will be a major contributor to the error.

Source positions will be obtained by comparison with field stars (~200 are expected to be detectable in one second on the average in the RMT field-of-view). With a pixel size of 1.8 arcsec and diffraction limit of 0.7 arcsec, it should be possible, in principal, to find the centroid of the transient source image to much better than 1 arcsec. The actual location errors will, however, be limited by the systematic tracking errors as well as seeing conditions. The time variability of the source will complicate the process of determining the true centroid of the image. Field tests will be necessary to determine whether or not the source can be located more precisely than the  $\pm 1$  arcsec

tracking error.

We calculate the RMT sensitivity as follows: Since our pixel size is 1.8 arcsec the sky background contribution is negligible, and we are hence limited by detector noise. The minimum detectable flux at significance level  $S$  (measured in no. of  $\sigma$ ) is given by:

$$\psi_S = \frac{SN}{A\tau\epsilon\Delta\lambda} \text{ (photons/cm}^2\text{-sec-}\Delta\lambda\text{)}$$

where

- $\epsilon$  = total optical throughput (electrons/photon)
- $\Delta\lambda$  = system passband in  $\text{\AA}$
- $A$  = telescope aperture ( $\text{cm}^2$ )
- $\tau$  = system integration time (seconds)
- $N$  = rms readout noise (electrons/pixel)

The apparent magnitude  $m$  is defined to be<sup>8</sup>

$$m = -2.5 \log f_\lambda - 21.1$$

where  $f$  is the energy flux in  $\text{ergs}/(\text{cm}^2\text{-sec-Angstrom})$ , i.e.  $f_\lambda = \psi \times \Delta\lambda E$ , where  $E$  is the average number of ergs/photon.

$$\text{For } \psi = \psi_S, m = -2.5 \log \left( \frac{SN\Delta\lambda}{A\tau\epsilon} \right) - 21.1.$$

For  $\epsilon = 0.5$  electrons/photon,  $S = 20$ ,  $N = 20$  electrons/pixel,  $\Delta\lambda = 4000\text{\AA}$  and  $\tau = 1$  second then  $m = 15.2$ .

In summary we have begun development of an instrument which has the capability of locating optical transient sources to sufficient accuracy to permit identification at the limiting magnitude of the largest ground-based telescope and eventually with Space Telescope as well. Operation in conjunction with the MIT-developed ETC is expected to begin at Kitt Peak in early 1985. These two instruments are opening a relatively untouched area in astronomy, namely the study of transient phenomena with time scales on the order of one second. It is entirely possible that new and unexpected results will be obtained.

#### REFERENCES

1. B. E. Schaefer, *Nature* 294, 722 (1981).
2. G. R. Ricker, J. P. Doty, J. V. Vallergera and R. K. Vanderspek, to be published, proceedings S.P.I.E. Conference (1983).
3. G. R. Ricker, J. P. Doty, J. V. Vallergera and R. K. Vanderspek, these proceedings (1983).
4. B. E. Schaefer, these proceedings (1983).
5. H. Pederson, C. Motch, M. Tarenghi, J. Danziger, G. Pizzichini, and W. H. G. Levin, *Ap. J.*, 270, L43 (1983).
6. B. E. Schaefer, P. Seitzer, and H. V. Brandt, *Ap. J.*, 270, L49, (1983).
7. H. Pederson et al., *Ap. J.*, 263, 325 (1982).
8. C. W. Allen, *Astrophysical Quantities*, Athlone Press, p. 197 (1976).